


ELECTROCHEMICAL DISSOLUTION OF ZnO SINGLE CRYSTALS


APPROVED:


Graduate Committee:


  
Major Professor


  
Minor Professor

  
Committee Member

  
Committee Member

  
Committee Member

  
Director of the Department of Chemistry

  
Dean of the Graduate School

ELECTROCHEMICAL DISSOLUTION OF ZnO SINGLE CRYSTALS

DISSERTATION

Presented to the Graduate Council of the  
North Texas State University in Partial  
Fulfillment of the Requirements

For the Degree of

DOCTOR OF PHILOSOPHY

By

David Dixon Justice, B. S.

Denton, Texas

January, 1970

## TABLE OF CONTENTS

	Page
LIST OF TABLES. . . . .	iv
LIST OF ILLUSTRATIONS . . . . .	v
Chapter	
I. INTRODUCTION. . . . .	1
II. ELECTROCHEMISTRY OF SEMICONDUCTORS . . . . .	21
III. PREVIOUS EXPERIENCE IN ELECTROCHEMISTRY AND DISSOLUTION OF ZnO. . . . .	50
IV. EXPERIMENTAL. . . . .	58
V. DATA . . . . .	69
VI. CONCLUSION . . . . .	95
Passivity Phenomenon Hydrogen Gas Evolution Capacity Measurements Photovoltage Dissolution Rates Proposed Dissolution Mechanism	
BIBLIOGRAPHY . . . . .	109

## LIST OF TABLES

Table	Page
I. Physical Properties and Dimensions of ZnO Single Crystals . . . . .	58
II. Summary of Dissolution Rates . . . . .	86
III. Comparison of Weight of Zinc Found Experi- mentally to Weight of Zinc Expected from Current Measurements. . . . .	87

## LIST OF ILLUSTRATIONS

Figure	Page
1. Bridging Routes between Metallic and Insulating Bonds . . . . .	3
2. Charge Distribution around the Interface between a Metal and an Electrolyte . . . . .	7
3. Potential Distribution in the Double Layer . . . . .	8
4. Formation of a Mixed Potential . . . . .	10
5. Dependence of Anodic ( $U_+$ ) and Cathodic ( $U_-$ ) Activation Energies on Overpotential ( $\eta$ ) . . . . .	14
6. Electron Energy Diagram for an N-Type Semiconductor . . . . .	23
7. Electron Energy Diagram for a P-Type Semiconductor . . . . .	24
8. Fermi Distribution Function for a Metal . . . . .	26
9. Fermi Distribution for an Intrinsic Semiconductor. . . . .	27
10. Relative Position of Fermi Energy in an N-Type Semiconductor . . . . .	28
11. Relative Position of Fermi Energy Level in a P-Type Semiconductor . . . . .	29
12. Energy Level Diagram for an N-Type Semiconductor-Solution Interface under Conditions of Bands Bending Up. . . . .	30
13. Energy Level Diagram for an N-Type Semiconductor-Solution Interface under Conditions of Bands Bending Down . . . . .	31
14. Charge Distribution around the Semiconductor-Solution Interface. . . . .	33
15. Space-Charge Capacity as a Function of Potential, . . . . .	35

16.	Potential Distribution around a Semi-conductor-Solution Interface . . . . .	37
17.	Representation of Mixed Potential ( $U_M$ ) on ZnO in an Alkaline Solution. . . . .	38
18.	Open Circuit Potential of ZnO in 1 N KOH as a Function of Relative Light Intensity. . . . .	39
19.	Correlation of Silicon Dissolution Rate with Current-Voltage Relation . . . . .	47
20.	Apparatus for Producing ZnO Single Crystals.	51
21.	Representation of Crystal Lattice of ZnO. . . . .	53
22.	Profile of a ZnO Surface . . . . .	54
23.	Electrical Contact to ZnO Single Crystal. . . . .	60
24.	Representation of ZnO Face . . . . .	61
25.	Schematic Diagram of Electrochemical Cell . . . . .	63
26.	Schematic Diagram of Circuit Used to Maintain a Constant Potential . . . . .	64
27.	Working Curve Relating Absorbance to Concentration for a Routine Zinc Analysis . . . . .	66
28.	Potential-Time Response of a 2.0 ohm-cm ZnO Crystal in 1 N KOH . . . . .	70
29.	Dissolution Rates as a Function of Potential for the Zinc Face of an 8.5 ohm-cm ZnO Crystal in the Dark in 1 N KOH. . . . .	72
30.	Correlation of Zinc Dissolution Rates with the Current-Voltage Relation . . . . .	73
31.	Potential-Time Response of a 2.0 ohm-cm ZnO Crystal in Alkaline Solutions upon Irradiation . . . . .	75
32.	Dissolution Rates as a Function of Potential for the Zinc Face of an 8.5 ohm-cm ZnO Crystal in 1 N KOH in Light. . . . .	77
33.	Correlation of Zinc Dissolution Rates with the Current-Voltage Relation . . . . .	78

34.	Dissolution Rates as a Function of Potential for the Zinc Face of a 2.0 ohm-cm ZnO Crystal in 0.5 N KOH in Light . . . . .	80
35.	Correlation of Zinc Dissolution Rates with the Current-Voltage Relation in 0.5 N KOH. . . . .	81
36.	Dissolution Rates as a Function of Potential for the Zinc Face of an 8.5 ohm-cm ZnO Crystal in 0.5 N KOH in Light . . . . .	83
37.	Correlation of Zinc Dissolution Rates with the Current-Voltage Relation in 0.5 N KOH. . . . .	84
38.	Comparison of Anodic Current-Voltage Curves of ZnO Single Crystal Electrodes . . . . .	88
39.	Potentiostatic Current-Voltage Curves. . . . .	90
40.	Comparison of Cathodic Current-Voltage Curves of ZnO Electrodes. . . . .	92
41.	Effect of Light upon Potential-pH Curves of ZnO Electrodes . . . . .	93
42.	Photomicrograph of Zinc Face of Single Crystal ZnO after Exposure to 1 N KOH . . . . .	94
43.	Effect of Resistivity upon the Linear Relation between the Square of Current vs Potential. . . . .	103

## CHAPTER I

### INTRODUCTION

Dissolution of the ionic crystalline state to form solvated ions involves oxidation-reduction reactions for metallic conductors, surface solvation and bond breaking for insulators, and probably some of each for semiconductors. The separation of oxidation-reduction reactions into individual half-cells with a resulting "mixed potential" is well known as a dissolution mechanism for metals; however, the mechanism by which non-conducting crystals lose ions to the solution has been studied only slightly. These processes are thought to involve the adsorption of ions from solution onto the surface of ionic crystals and the establishment of localized electrical fields by these ions (8); the localized electrical fields force either a cation or anion into solution; then the ion of opposite charge quickly leaves the crystal lattice so that electrical neutrality is maintained. The dissolution processes occurring on substances that bridge the "conductivity gap" between conductors and insulators (semiconductors) have been studied even less than the processes occurring on ionic crystals; however, from the work that has been done with semiconductors, the existence of oxidation-



reduction steps has been clearly demonstrated on germanium (1) and silicon (5) in aqueous alkaline solutions.

Atoms of the elemental semiconductors, germanium and silicon, are held together in single crystals by covalent bonds; thus, these can be thought of as forming a bridge between metal conductors and covalent insulators. Compound semiconductors have bonding structures that range from almost completely covalent to almost completely ionic. An indication of the degree of ionic and covalent character is given by the Sziget parameter (7), which has a value of one for purely ionic substances and zero for purely covalent substances. Of the few Sziget parameters determined, MgO, which for all practical purposes is an ionic insulator, has a Sziget parameter of 0.88 (7, p. 163); ZnS has a value of 0.48 (7, p. 163), and ZnO has a value of 0.63 (3, p. 578). Presumably a semiconductor such as Bi<sub>2</sub>Te<sub>3</sub> would have a Sziget parameter of less than 0.48. The difference in electronegativities for magnesium and oxygen is 2.3; the difference for zinc and sulfur is 1.0; for zinc and oxygen it is 2.0, and for bismuth and tellurium it is 0.2. Loosely based upon Sziget parameters and electronegativity differences, ZnO can be thought of as an "intermediate" with respect to ionic or covalent character and thus can be thought of as forming a type of bridge between metal conductors and ionic insulators; thus, there are two "bridging

routes" between metallic and insulating bonds. In addition to the previously established route through germanium and silicon, there is now with the conclusion of the present work a route through the compound semiconductor, ZnO, as shown in Figure 1. Because ZnO is available in the form of reasonably large single crystals, it has been the most widely studied and best understood of the compound semiconductors; however, the mechanism of dissolution in aqueous solutions is not clearly understood even for ZnO.

Since oxidation-reduction reactions occurring during the dissolution of pure metal conductors are potential dependent (electrochemical dissolution) while surface solvation and bond breaking occurring during insulator dissolution are potential independent (chemical dissolution), a study of the dissolution rates of single crystal ZnO as a function of potential can be used to determine whether this particular compound semiconductor dissolves by an electrochemical, chemical, or a combination electrochemical-chemical mechanism. Since electrochemical principles have been well established,

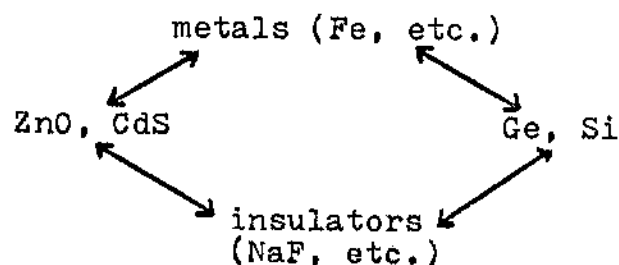


Fig. 1--Bridging routes between metallic and insulating bonds.

the purpose of this investigation was to determine whether or not the dissolution rates of ZnO single crystals were a function of potential and, if a potential dependency were found, to measure the dissolution rates as a function of potential and correlate them with existing theories of electrochemical dissolution (taking into consideration the special properties characteristic of semiconductors). It was hoped that this work would not only determine a dissolution mechanism which could explain the processes occurring on ZnO but might also provide an indirect path for a better understanding of the dissolution mechanism of ionic crystals.

For eventually discussing semiconductor principles, it is easier and perhaps more unifying to think of bonding not in terms of covalent or ionic bonds but in terms of energy bands which constitute the allowed electronic energy levels of crystalline solids. In this energy band model, there is a close distribution of energy levels, termed the valence band, which is lower in energy than and separate from a second close distribution of possible electronic energy levels, termed the conduction band. In the region between the two bands there is a very low probability for the existence of energy levels; consequently, this region is termed the forbidden gap. From the point of view of conduction phenomena in metals, insulators, and semiconductors, the important point is that electrons can be accelerated by

an external field and thus contribute to an electric current only if they are moving in a partially empty band (4, p. 30).

Metals have valence electrons that lie either in unfilled bands (the one 3s electron in sodium) or in filled bands that overlap with empty bands (the 3s and 3p overlap for the two 3s electrons of magnesium). Metals can be thought of as a positive ion lattice (a filled underlying band) surrounded by a "sea of electrons" in which the electrons are not associated with any particular atom but are free to move under the influence of an applied electrical field (unfilled conduction band). In metals, charges are carried only by electrons; the number of electrons in the conduction band is very high compared to the number in the conduction bands of insulators and semiconductors. For insulators the valence band is filled; the conduction band is empty, and the forbidden gap is so large there is only an extremely small probability of electrons from the valence band having enough thermal energy at room temperature to make the transition to the conduction band; thus, essentially all the electrons are localized in a filled valence band, and the conductivity for insulators is very low. For semiconductors the energy gap between the valence and conduction bands is much smaller than for insulators; therefore, there is a higher probability of electrons from the valence band having enough thermal

energy at room temperature to be delocalized and to exist in the conduction band; however, the distributions are such that the delocalized electron density of semiconductors is much less than that of metals.

Even though there are a very few cases reported (2, 6) in which an adsorbed species on the surface of the metal can localize electrons from the conduction band of the metal into overlapping orbitals of the adsorbed species to form a layer of ionic compound between the electrolyte and the metal, in which case the dissolution process involves just the chemical dissolution of the ionic compound layer, most metal dissolution processes are electrochemical in nature. An understanding of the electrochemical processes occurring on metal electrodes can, in many cases, be extended to explain phenomena occurring at semiconductor electrodes.

When a metal is placed in an electrolyte, there is an exchange of electrons between the metal and the ions in solution until an equilibrium is established. The discharge of an ion from solution involves at least two stages; the solvated ion in the bulk of the solution is transferred to the electrode surface; then the adsorbed ion combines with an electron provided by the electrode and is discharged. In the reverse process an atom of the metal loses one or more electrons and is then transferred into the bulk of the solution.

At equilibrium the forward and reverse reactions occur at the same rate; this is a dynamic equilibrium, and no net flow of current occurs. The charges being transferred between the metal-electrolyte phases result in layers of excess charges at the metal-electrolyte interface, as shown in Figure 2.

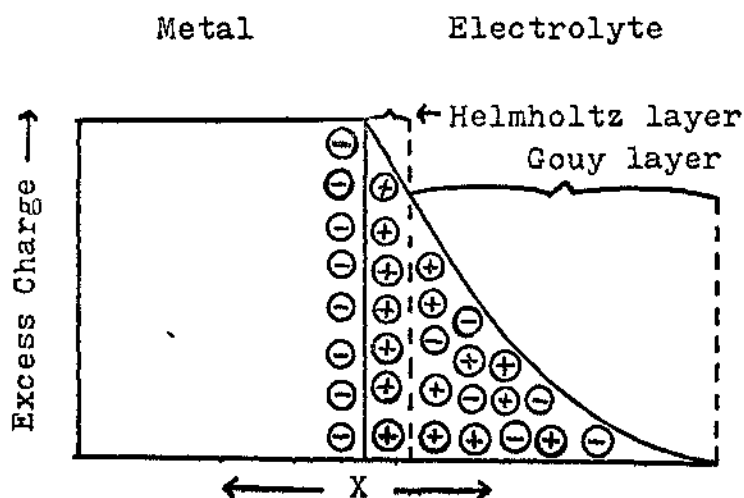


Fig. 2--Charge distribution around the interface between a metal and an electrolyte; (X) distance from the metal surface.

This charge distribution is called the double layer; from the solution viewpoint it can be described as having the charge divided into a surface charge formed by close-packed ions (Helmholtz layer) and a space charge region in which the charge is distributed many ion diameters into the electrolyte (Gouy layer). On the metal electrode side all the excess opposite charge is located within a few angstroms of the surface. Within the metal the potential distribution is essentially

constant from the metal bulk to the surface, but in the electrolyte the magnitude of the potential decreases exponentially, as shown in Figure 3.

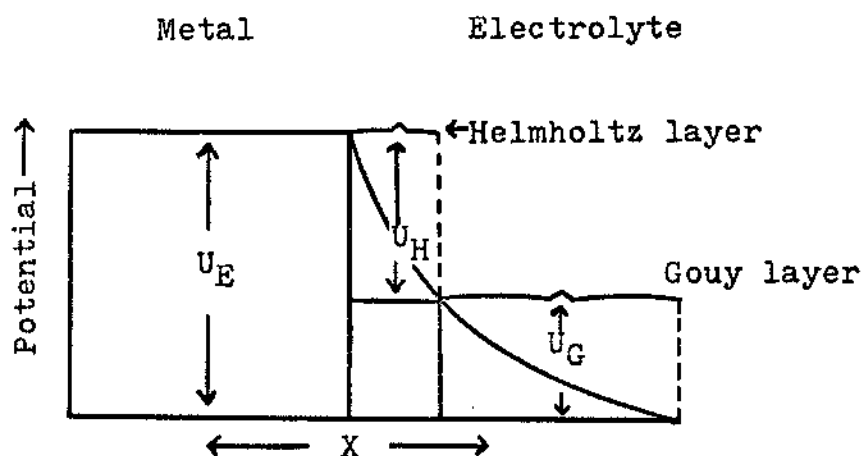


Fig. 3--Potential distribution in the double layer: ( $U_E$ ) potential difference, ( $U_H$ ) potential drop across the Helmholtz layer, ( $U_G$ ) potential drop across the Gouy layer, ( $X$ ) distance from metal surface.

Since the excess charge of the metal is located very close to the surface, electrochemical reactions at metal electrodes are determined entirely by phenomena occurring in the solution or at the solution-metal interface. The potential gradient across the solution-metal interface is a determining factor in the rate of the electrochemical reactions that make up the corrosion reaction; this will be discussed in more detail later.

The dissolution of iron in acidic solution can be used as an example to further develop these concepts. When an iron electrode is placed in an acid solution, it would attain an equilibrium potential if only one

reaction ( $\text{Fe}^0 \rightleftharpoons \text{Fe}^{+2} + 2e'$ ) occurred; however, in reality two or more different electrode reactions occur independently of each other on the metal surface. For an iron electrode these independent reactions are the anodic oxidation of iron ( $\text{Fe}^0 \rightarrow \text{Fe}^{+2} + 2e'$ ) and the cathodic reduction of solvated hydrogen ions ( $2\text{H}^+ + 2e' \rightarrow \text{H}_2$ ). The oxidation of iron accompanied by the corresponding evolution of hydrogen is termed the corrosion of iron. An absolute value for the equilibrium potential of either one of these electrode reactions can not be measured; however, with appropriate circuitry and electrode conditions, changes in the one interfacial potential that is important to corrosion kinetics can be measured; thus, for iron the change in potential that is of interest is not that of either the  $\text{Fe}/\text{Fe}^{+2}$  or  $\text{H}^+/\text{H}_2$  reaction but is the one that is set up by the sum of the thermodynamic properties of both the  $\text{Fe}/\text{Fe}^{+2}$  and the  $\text{H}^+/\text{H}_2$  reactions. This net potential is called the "mixed potential".

When no external potential is applied to the iron electrode, the system is at "open circuit" conditions. Anodic and cathodic processes are occurring, but the magnitudes of the currents for these two "half-cell reactions" (termed the corrosion current,  $i_{\text{corr}}$ ) are equal but opposite in sign ( $i_+ = i_- = i_{\text{corr}}$ ) so that the net current is zero. If an additional electrical potential is imposed between the iron electrode and a



second electrode (termed polarization of the electrode), the magnitudes of the currents for the two half-cell reactions are no longer equal, and an appreciable current can flow from the electrode to solution or vice versa. As shown in Figure 4, the anodic half-cell current increases with anodic polarization whereas the cathodic current decreases; under cathodic polarization the cathodic current increases while the anodic current decreases.

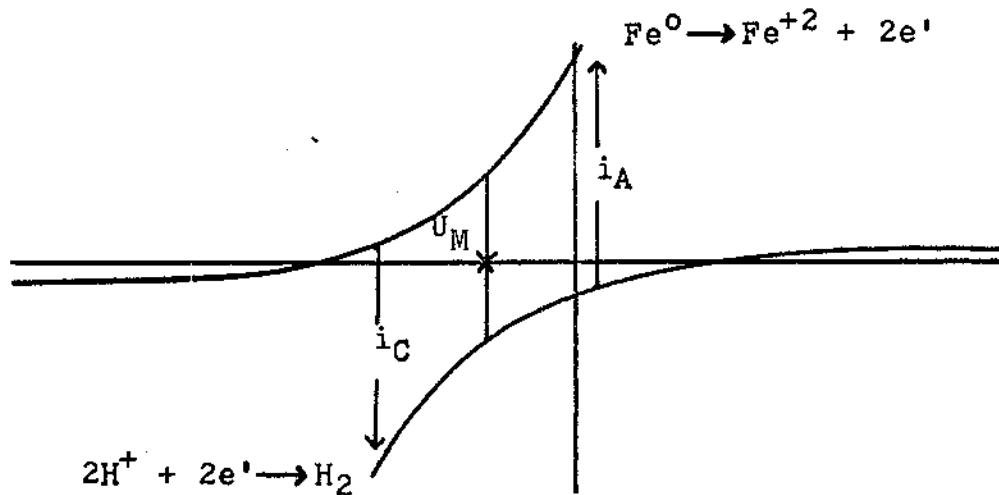


Fig. 4--Formation of a mixed potential: ( $U_M$ ) mixed potential, ( $i_A$ ) anodic polarization current, ( $i_C$ ) cathodic polarization current.

This imposed potential, called "overpotential" ( $\eta$ ), is a function of current density (current per  $\text{cm}^2$  of electrode area). The formation of this current controlled polarization or overpotential originates in the hindrance of the overall electrode reaction (9, p. 105) which itself is composed of a series of five

partial reactions. This can be summarized by the following expression:

$$\eta_T = \eta_{\text{trans.}} + \eta_{\text{rx.}} + \eta_{\text{diff.}} + \eta_{\text{crystal}} + \eta_{\text{resist.}}$$

(Eq. 1)

$\eta_T$  is the total overpotential.  $\eta_{\text{trans.}}$  is the overpotential due to the transfer of charge carriers across the electrical double layer being a slow step in the partial reactions, and  $\eta_{\text{rx.}}$  is the overpotential due to a slow step being a chemical reaction.  $\eta_{\text{diff.}}$  is the overpotential caused by a slow step being the mass transport diffusion to and from the surface of substances formed or consumed during the reaction. (The reaction and diffusion overpotentials are usually considered to be combined together in a concentration overpotential.)  $\eta_{\text{crystal}}$  is the overpotential due to a slow step being the incorporation of atoms into or the removal of atoms out of the crystal lattice, and  $\eta_{\text{resist.}}$  is the overpotential due simply to a current flowing through a resistance.

Usually the resistance overpotential is not included in the total overpotential because it is described as the ohmic potential drop within the electrolyte; that is, it is the additional potential needed to overcome the resistance of the electrolyte to the passage of a certain current. This assumes there is no IR drop in the metal itself. Since metal conductors have large numbers of electrons which readily permit a current flow, the metal

presents very little resistance to a current and thus has very little IR drop. This is not true for semiconductors because there are fewer delocalized charge carriers; thus, the resistance of the semiconductor itself is much higher, and a large IR drop can occur within the semiconductor; therefore, resistance overpotential can be very important for semiconductors.

Usually only one of the five partial reactions is slower than the others and thus controls the overall electrode reaction rate; this rate determining step can usually be determined by varying the experimental conditions and by determining current versus potential plots for the electrode. For example, if the overall electrode reaction rate is diffusion controlled, the diffusion overpotential decreases with an increase in stirring, or if the reaction rate for a metal electrode is resistance controlled, the IR drop in the electrolyte can be made smaller by increasing the concentration of the electrolyte and by moving the reference electrode closer to the metal electrode.

Of the partial reactions, only the transition overpotential is directly dependent on potential; thus, an electrochemical reaction is a reaction in which at least one of the partial reactions involves the transfer of charge carriers across the electrical double layer at a phase boundary. The effect of other variables on the potential are seen indirectly by the manner in which

these variables influence the transition overpotential (9, p. 107). The overpotential is related to the transition reaction by the manner in which the overpotential influences the heights of the activation energies of the anodic and cathodic half-cell reactions. Whereas the chemical activation energy is a relatively constant value, the electrochemical activation energy is composed of a chemical activation energy term plus a potential dependent term. A descriptive understanding of the process can be obtained with the help of the energy diagrams shown in Figure 5.

Curve A of Figure 5 represents the energy changes occurring in the double layer when there is no imposed potential and can, therefore, be thought of as the "chemical energy" curve. Curve B represents an imposed potential, that is, an overpotential. The magnitude of this overpotential can be expressed as an energy term,  $ZF\eta$ , where  $Z$  is the number of equivalents per mole,  $F$  is a faraday, and  $\eta$  is the overpotential. Curve C is an additive superimposition of curves A and B; therefore, curve C indicates the changes in "electrochemical" energy as a function of distance at some value of the overpotential not equal to zero.

Of the total electrochemical energy added, only a part of it,  $\alpha ZF\eta$  (where  $\alpha$  is the transfer coefficient which can have any value between zero and one) affects the anodic activation energy, and the remainder,  $(1-\alpha)$

$ZF\eta$ , affects the cathodic activation energy. When electrical energy is added by imposing an anodic overpotential, the anodic activation energy is lowered and the cathodic activation energy is increased; under cathodic polarization the anodic activation energy is increased and the cathodic activation energy decreased.

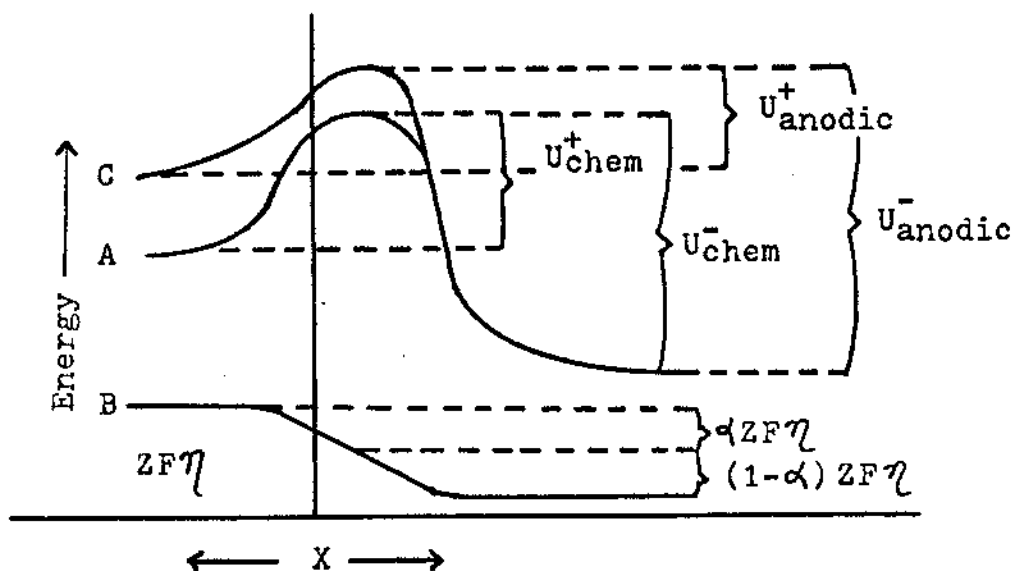


Fig. 5--Dependence of anodic ( $U_+$ ) and cathodic ( $U_-$ ) activation energies on overpotential ( $\eta$ ); (X) distance from the surface, (A) chemical energy curve, (B) applied potential, (C) electrochemical energy curve.

For a first order chemical reaction the rate can be given in terms of the transition-state theory by the following expression:

$$\frac{dN_A}{dt} = \frac{kT}{h} C_A e^{-\Delta G_0/RT} \quad (\text{Eq. 2})$$

where  $dN_A$  is the change in concentration of species A,  $dt$  is the change of time,  $k$  is Boltzmann's constant,  $T$  is the absolute temperature,  $h$  is Planck's constant,  $C_A$  is the concentration of species A,  $\Delta G_0$  is the change of free energy in the standard state, and  $R$  is the universal gas constant.

For a general electrochemical reaction in which only one reaction occurs (Oxid. +  $Ze' \xrightleftharpoons[k_+]{k_-}$  Red.) the anodic ( $k_+$ ) and cathodic ( $k_-$ ) "rate constants" vary with potential; therefore, the rate expression has to be written in the form of two half-cell rate expressions as given by the following equations:

$$-\frac{dN_{\text{red.}}}{dt} = k_+ C_{\text{red}} e^{\frac{-\Delta G_+ + \alpha ZF\epsilon}{RT}} \quad (\text{Eq. 3})$$

$$-\frac{dN_{\text{oxid}}}{dt} = k_- C_{\text{oxid}} e^{\frac{-\Delta G_- - (1-\alpha)ZF\epsilon}{RT}} \quad (\text{Eq. 4})$$

where  $\epsilon$  is the absolute, unknown potential,  $\Delta G_+$  is the anodic activation energy,  $\Delta G_-$  is the cathodic activation energy, and the other terms have their usual significance.

By multiplying by  $F$  (96,450 coulombs per faraday) times  $Z$  (number of equivalents per mole) the rate can be expressed as a current in the following manner;

$$i_+ = -ZF \frac{dN_{\text{red}}}{dt} \quad (\text{Eq. 5})$$

$$i_- = -ZF \frac{dN_{\text{oxid}}}{dt} \quad (\text{Eq. 6})$$

where  $i_+$  is the anodic current, and  $i_-$  is the cathodic current.

At the equilibrium potential ( $\epsilon^0$ ), the following expressions are equal:

$$\begin{aligned} i_+ = i_- = i_o &= +ZFk_+ C_{\text{red}} e^{\frac{-\Delta G_+ + \alpha ZF\epsilon^0}{RT}} \\ &= +ZFk_- C_{\text{oxid}} e^{\frac{-\Delta G_- - (1-\alpha)ZF\epsilon^0}{RT}} \quad (\text{Eq. 7}) \end{aligned}$$

where  $i_o$  is the exchange current which is a kinetic parameter used to give a measure of the rate of equilibrium potential formation and of the sensitivity of the equilibrium potential to interferences such as applied potentials.

At any potential ( $\epsilon$ ), except the equilibrium potential ( $\epsilon^0$ ), the net current is equal to the absolute difference between the anodic and cathodic currents; the absolute difference between the unmeasurable potentials ( $\epsilon$ ) and ( $\epsilon^0$ ) is equal to the measurable overpotential ( $\eta$ ). After substituting and collecting terms, the following expression is obtained:

$$i_{\text{net}} = +i_o \left[ e^{\frac{+\alpha ZF\eta}{RT}} - e^{\frac{-(1-\alpha)ZF\eta}{RT}} \right] \quad (\text{Eq. 8})$$

At high overpotentials (50 millivolts or greater),  $|\eta| \gg \frac{RT}{\alpha ZF}$  or  $|\eta| \gg \left(\frac{1}{1-\alpha}\right) \frac{RT}{ZF}$  and one of the exponentials can be dropped. This gives the following linear dependence of overpotential on the logarithm of

the current (the Tafel equation):

$$\ln i = \ln i_0 + \frac{\alpha ZF\eta}{RT} \quad \text{or} \quad \ln/i/ = \ln i_0 - \frac{(1-\alpha)ZF\eta}{RT} \quad (\text{Eq. 9})$$

When plotted, the slope can be used to find  $\alpha$ , and the intercept gives a value for the exchange current. With the corrosion of metals, as mentioned earlier, there are two such electrochemical half-cell reactions involved; each has its own  $i_0$  and  $\alpha$  values. At zero polarization for the corroding metal, each of these reactions is already polarized to "high" overpotentials; extrapolation of the current-voltage curve for such a system gives values for a corrosion current rather than an exchange current. The corrosion current is related through Faraday's laws to the corrosion rate.

The same principles apply to semiconductors as well as to metals. An important point to be seen from the Tafel relation is that the magnitude of the corrosion current controls the amount of overpotential needed to force a certain amount of current through the electrode. Metals have much larger corrosion currents than semiconductors; for example, Fe in 1 N KOH may have an  $i_{\text{corr}}$  value of 100 milliamperes per  $\text{cm}^2$  while ZnO in 1 N KOH may have an  $i_{\text{corr}}$  value of 10 microamperes per  $\text{cm}^2$ . If it is desired to pass one ampere per  $\text{cm}^2$  through the circuit, five times the overpotential is needed for the ZnO electrode as for the iron.



The Tafel plot is widely used in studying metal electrode kinetics; however, it should be applied very cautiously to semiconductor electrode processes because three or four orders of magnitude between the corrosion current and a limiting current are needed to establish a Tafel region; this criterion is often not met with semiconductor electrodes because the bulk properties of semiconductors are different from those of metals; these differences are reflected in much lower conductivity values for semiconductors and in a charge distribution in semiconductors that is more like the solution phase of the double layer than the metal phase. This different type of charge distribution can greatly influence semiconductor electrode reactions. Bulk properties also permit the possibility that semiconductor reactions can proceed not only by the higher energy electrons in the conduction bands (as in metals) but also by "holes" in the lower-lying valence bands. As will be discussed in the following chapter, the electrochemical behavior of reactions in which holes participate is significantly different from the behavior when only electrons are involved. In addition it is possible to raise or lower the energy levels of the conduction and valence bands so that one or the other band "matches" the proper energy levels of a species in solution so that a reaction can occur between the species

and the semiconductor. These concepts are developed in more detail in Chapter II.

Capacity measurements, polarization data, and dissolution rates have been used to formulate and confirm dissolution mechanisms for the processes occurring on metal electrodes. In the following chapter it will be shown that the same types of data can also be determined for semiconductor systems, and even though the data are more difficult to interpret, they can still be very useful in studying the processes occurring during the dissolution of semiconductors.

## CHAPTER BIBLIOGRAPHY

1. Brattain, W. and Garrett, C., "The Interface Between Germanium and an Electrolyte," The Bell System Technical Journal, XXXIV (January, 1955), 129-177.
2. Florianovich, G. M. and Kolotyркиn, Y. M., "On the Problem of the Mechanism of the Solution of Iron Alloys with Chromium in Sulfuric Acid," Doklady Akademii Nauk SSSR, CLVII (July, 1964), 422-425.
3. Hannay, N. B., Semiconductors, New York, Reinhold Publishing Corporation, 1959.
4. Henisch, H. K., Rectifying Semiconductor Contacts, Oxford, Oxford University Press, 1957.
5. Hurd, R. and Wrotenbery, P., "Electrochemistry of the Silicon-Electrolyte Interface," Annals of the New York Academy of Sciences, CI (January, 1963), 876-903.
6. Oakes, G. and West, J. M., "Influence of Thiourea on the Dissolution of Mild Steel in Strong Hydrochloric Acid," British Corrosion Journal, IV (March, 1969), 66-73.
7. Szigeti, B., "Polarizability and Dielectric Constant of Ionic Crystals," Faraday Society Transactions, XLVIII (January, 1949), 155-166.
8. Vermilyea, D. A., "The Dissolution of Ionic Compounds in Aqueous Media," Journal of the Electrochemical Society, CXIII (October, 1966), 1067-1070.
9. Vetter, K. J., Electrochemical Kinetics, Theoretical and Experimental Aspects, New York, Academic Press, 1967.

## CHAPTER II

### ELECTROCHEMISTRY OF SEMICONDUCTORS

At absolute zero, electrons occupy the lowest possible energy levels; thus, in a semiconductor they completely fill the valence band and leave the conduction band vacant. At temperatures above absolute zero the distribution of electron energies is altered by thermal energy so that some of the higher energy electrons have a favorable probability of possessing enough energy to "jump" the forbidden gap to the conduction band. The number of electrons activated into the conduction band is a function only of temperature; for a pure material (intrinsic) the density of electrons in the conduction band is equal to the density of vacant covalent orbitals (holes) left in the valence band by the activated electrons. The density of holes or electrons can be altered by the addition of certain impurity species; this type of impurity semiconductor is termed extrinsic; this alteration of electron and hole densities by impurities is a result of the lattice structure and bonding of the semiconductor. For example, each germanium atom possesses four valence electrons in a tetrahedral configuration. Each atom is bonded to four other atoms

by covalent bonds in a bonding structure analogous to that of carbon in diamond. There is only a small density of vacant covalent orbitals in the valence band and the same small density of electrons in the conduction band. During the preparation of germanium single crystals, controlled amounts of impurities can be added to the molten state. When crystals are formed, these impurities take the place of some of the germanium atoms in the lattice bonding network. An element (arsenic) which has electrons not required in the bonding system of the lattice can be selected as one type of impurity. If this impurity is carefully selected so that it has a high probability of ionizing at room temperature, its presence can greatly increase the density of electrons in the conduction band; the density of electrons in the conduction band then depends upon the concentration of impurity added to the semiconductor. Since impurity atoms easily donate electrons to the conduction band, they can be pictured as having energy levels (donor levels) which lie in the forbidden gap close to the bottom of the conduction band. From another viewpoint the energy gap between the impurity donor atoms and the conduction band is smaller than the thermal energy of the excess electrons; thus, most of the electrons not involved in the covalent bonding network are easily activated to the conduction band. The positions of the energy levels are represented

pictorially in Figure 6 for this n- (negative) type of extrinsic semiconductor. Other impurities (indium) which need one or more electrons to complete the bonding system of the germanium lattice can also be substituted for some of the germanium atoms. The impurity can be carefully selected so that it has a high probability at room temperature of removing an electron from a neighboring covalent bond to satisfy its own bonding requirements. When the impurity accepts an electron, a vacant covalent orbital (hole) is left in a neighboring covalent bond. Another neighboring electron can fill this vacant orbital, but then another vacancy is created. This hole can migrate through the crystal and has all the properties expected of valence bond migration. Since this type of impurity easily accepts an electron at room temperature, it is pictured as having acceptor energy levels which lie close to but a little above the valence band energies, as illustrated

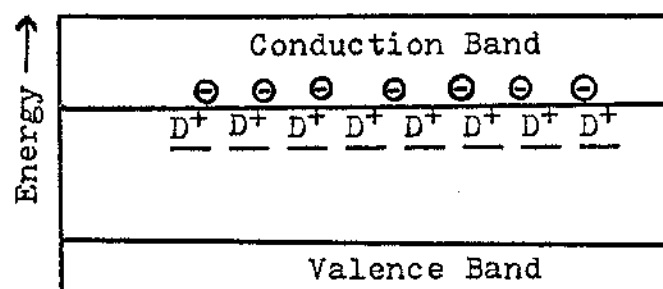


Fig. 6--Electron energy diagram for an n-type semiconductor: ( $D^+$ ) ionized donor atom, ( $\ominus$ ) electron donated to the conduction band by a donor atom.

in Figure 7. This type of semiconductor is called a p- (positive) type because the principal source of conduction is holes in the valence band; in the presence of an applied electric field these holes move in the opposite direction from that of conduction electrons. Conduction in a semiconductor then occurs by negative charges (electrons) in the conduction band and by positive charges (holes) in the valence band.

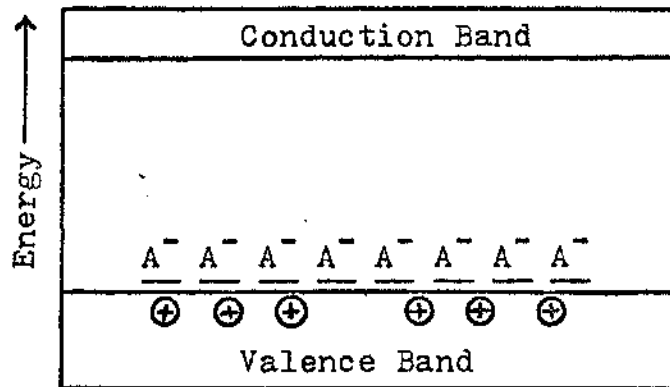


Fig. 7--Electron energy diagram for a p-type semiconductor: ( $A^-$ ) ionized acceptor atom, ( $\oplus$ ) delocalized hole left in the valence band by the loss of an electron from the valence band to an acceptor atom.

Electrons in a semiconductor follow the Fermi-Dirac distribution law which can be expressed as follows:

$$f(E) = \frac{1}{1 + \exp \frac{(E-E_F)}{KT}} \quad (\text{Eq. 10})$$

where  $f(E)$  is the probability that a state of energy  $E$  is occupied,  $E_F$  is the Fermi energy which is that energy

level at which the probability of the level being occupied by an electron is  $\frac{1}{2}$ ,  $k$  is Boltzmann's constant, and  $T$  is the absolute temperature. At absolute zero all electrons are in the lowest energy states, and  $E_F$  is the energy associated with the highest occupied states as shown by curve A of Figure 8. In other words, at absolute zero the probability that energy states below the Fermi level are occupied is one, and the probability that energy states above the Fermi level are occupied is zero. As the temperature is increased, the probability that energy states much, much below the Fermi level are occupied is still one, and likewise for energy states much, much above the Fermi level, the probability is still zero; however, in the energy states close to the Fermi level, changes occur in the electron occupancy distribution. Some electrons have enough thermal energy to occupy energy states above the Fermi level; consequently, there is a rounding off of the distribution function in the neighborhood of the Fermi level as illustrated by curve B of Figure 8.

For metals at absolute zero, all the electrons occupy the lowest energy states, but there is a continuum of energy states in a metal; therefore, as the temperature is raised, very little energy is needed for an electron to occupy a slightly higher energy state. For a semiconductor at absolute zero, all the electrons again occupy the lowest energy states (the valence band),



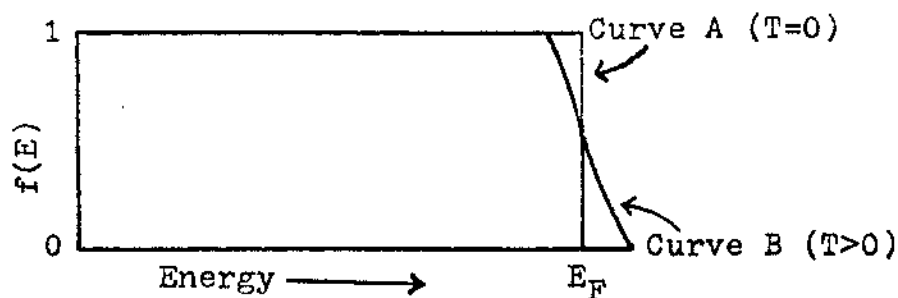


Fig. 8--Fermi distribution function for a metal: ( $f(E)$ ) probability that a state of energy  $E$  is occupied, ( $E_F$ ) Fermi energy level.

but there is not a continuum of energy states immediately above the occupied states because the forbidden gap separates the lower energy valence band from the conduction band. As the temperature is increased, an electron can not acquire a small amount of thermal energy to slip into a close lying energy continuum but must possess enough thermal energy to be activated across the forbidden gap to the conduction band. This means that the Fermi level for a semiconductor can not be represented as coinciding with the highest occupied energy state at absolute zero but has to be represented as being between the valence and conduction bands. For an intrinsic semiconductor the density of electrons in the conduction band and holes in the valence band is equal, and the Fermi level can be represented as being midway between the two bands, as shown in Figure 9. For an extrinsic semiconductor there is an additional donor

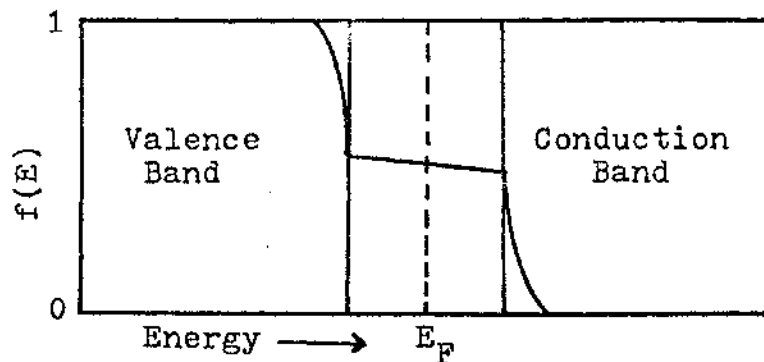


Fig. 9--Fermi distribution for an intrinsic semiconductor: ( $f(E)$ ) probability that a state of energy  $E$  is occupied, ( $E_F$ ) Fermi energy level.

or acceptor level between the two bands. For an n-type semiconductor at absolute zero, the valence band is filled; the donor atoms are unionized, and the conduction band is empty. There is a small energy gap between the donor levels and the conduction band; this energy gap is smaller than the forbidden gap in intrinsic semiconductors but still much larger than the very small amounts of energy needed for a similar transition in metals. As the temperature is increased, electrons of the donor atoms acquire enough energy to be activated across the energy gap to the conduction band; consequently, the Fermi level for an n-type semiconductor is represented as being close to the donor level or between the donor level and the conduction band as shown in Figure 10. For a p-type semiconductor the valence band at absolute zero is again filled; the acceptor atoms are unionized, and the conduction band

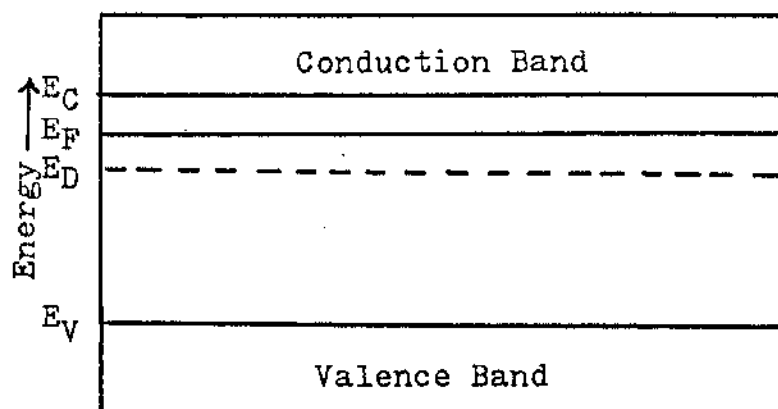


Fig. 10--Relative position of Fermi energy in an n-type semiconductor: ( $E_V$ ) upper edge of valence band energy levels, ( $E_D$ ) donor energy level, ( $E_F$ ) Fermi energy level, ( $E_C$ ) lower edge of conduction band energy levels.

is empty. Again there is a small energy gap between the valence band and the acceptor levels. As the temperature is increased, the acceptor atoms must attract the valence electrons across this energy gap; the Fermi level is represented as being close to the acceptor level or between the valence band and the acceptor levels, as shown in Figure 11.

Up to this point the discussion has been concerned mainly with the physics of semiconductors; the following paragraphs discuss the most important electrochemical aspect of semiconductors, namely the semiconductor surface region. The energy required for an electron to make the transition from the valence band to the conduction band (or from donor levels to the conduction band) can be provided in ways other than through  $kT$

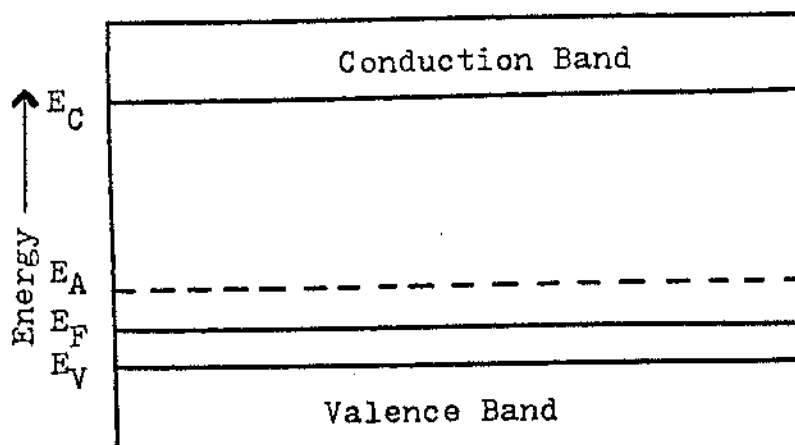


Fig. 11--Relative position of Fermi energy level in a p-type semiconductor: ( $E_V$ ) upper edge of valence band energy levels, ( $E_F$ ) Fermi energy level, ( $E_A$ ) acceptor energy level, ( $E_C$ ) lower edge of conduction band energy levels.

(thermal) energy. Of these there are two which are of particular pertinence to the present study with ZnO, namely the addition of energy through incident light of the proper wavelength on the surface region and through electrical energy applied to the bulk of the semiconductor when used as an electrode in an electrolytic circuit. A third method, which is often of interest to electrochemical work on semiconductors, is through the addition to the electrolyte of oxidizable or reducible substances which have a tendency to extract or inject electrons from or into the valence or conduction bands of surface atoms. In the presence of any of these external energy sources, the new energy band configuration can be represented pictorially by bending the energy bands up or down, depending on whether the

energy is increased or decreased. For example, ZnO is an n-type semiconductor, and when a ZnO single crystal electrode is placed in 1.0 N KOH, hydroxide ions influence the electron-hole distribution in the semiconductor so that the hole distribution is increased at the surface and the electron density is decreased, as shown in Figure 12. A similar bending could be obtained by applying anodic voltages. When the electron-hole distribution is altered so that the hole density at the surface is greater than the hole density in the bulk of the crystal while the electron density is smaller at the surface than in the bulk, a "depletion" layer is formed at the surface; that is, the majority current carriers (in ZnO these are electrons) are depleted at the surface. If the bands are bent upward until the hole density at

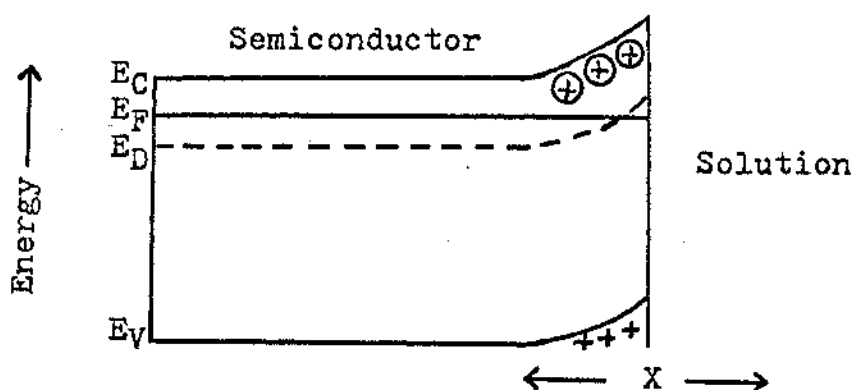


Fig. 12--Energy level diagram for an n-type semiconductor-solution interface under conditions of bands bending up (anodic polarization): ( $E_V$ ) upper edge of valence band energy levels, ( $E_D$ ) donor energy level, ( $E_F$ ) Fermi energy level, ( $E_C$ ) lower edge of conduction band energy levels, ( $X$ ) distance from surface, (+) excess holes at the surface, ( $\oplus$ ) ionized donor atoms at the surface.

the surface is larger than the electron density in the bulk, a so-called inversion layer is formed at the surface. If the bands are bent down, for example by cathodic polarization, the electron density at the surface becomes greater than the electron density in the bulk, and an enrichment (enrichment of the majority carrier at the surface) layer forms, as shown in Figure 13.

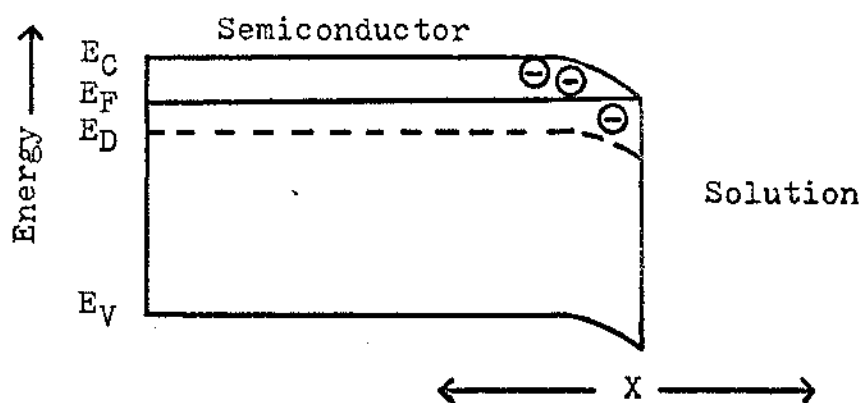


Fig. 13--Energy level diagram for an n-type semiconductor-solution interface under conditions of bands bending down (cathodic polarization): (X) distance from surface, ( $E_V$ ) upper edge of valence band energies, ( $E_D$ ) donor energy level, ( $E_F$ ) Fermi energy level, ( $E_C$ ) lower edge of conduction band energy levels, ( $\ominus$ ) excess electrons at the surface.

Since these energy bands can be bent by external means, it is possible to arrange experimental conditions so that there is no band bending; that is, there is a potential under certain experimental conditions at which the electron and hole densities at the surface are equal to the electron and hole densities in the bulk.

In electrochemical work with semiconductors this potential is called the "flat-band" potential.

When a semiconductor is placed in aqueous electrolytes, there is a more complicated double layer formed than the double layer formed at the metal-electrolyte interface. The solution part of the double layer is formed for the semiconductor in exactly the same way as it is for the metal; that is, there is a surface charge formed by close packed ions and then a diffuse double layer in which the charge is distributed many ion diameters into the electrolyte. The difference arises in the interior of the solid phase, specifically in the region near the interface. In the metal, electrons are highly mobile; energy levels are closely spaced, and the excess charge is then located within an angstrom or so of the surface. In a semiconductor the density of charge carriers is much smaller, and their mobilities are much lower. These differences cause the excess charges (either electrons or holes) of the semiconductor to be located not within an angstrom or so of the surface but spread out in a distribution from the surface to some extent inside the semiconductor, as shown in Figure 14. This charge distribution called the "space charge region" is more analogous to the charge distribution in electrolytes than the charge distribution in metals. The existence of this space charge region is extremely important

because electrochemical reactions can be influenced not only by phenomena occurring in the solution and at the semiconductor-solution interface but also by phenomena that occur within this space charge region.

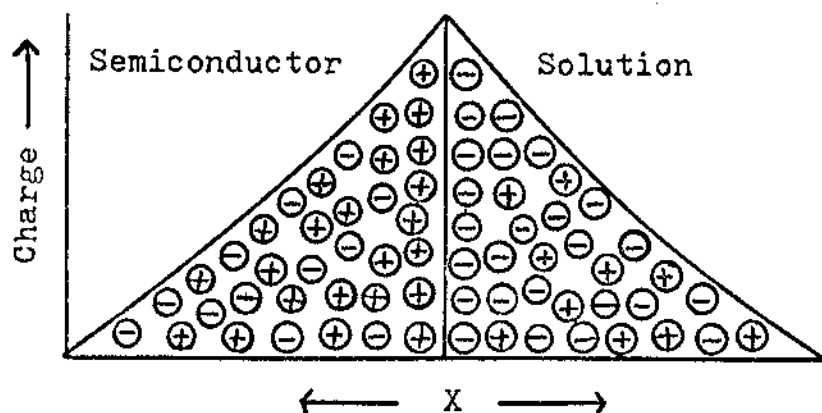


Fig. 14--Charge distribution around the semiconductor-solution interface: (X) distance from surface, (⊕) positive charges, (⊖) negative charges.

The semiconductor space charge region can be treated both conceptually and mathematically as a condenser; that is, a capacity can be determined for this region in analogy to the capacity of any condenser. Capacity (C) is defined as  $\frac{dQ_R}{dU_R}$  where  $Q_R$  is the surface charge density, and  $U_R$  is the potential drop across the space charge region. For a semiconductor-electrolyte interface the total capacity ( $C_T$ ) of the electrolyte can be thought of as the capacity of the close-packed ions ( $C_H$ ) in series with the capacity of the diffuse double layer ( $C_G$ ). Both



of these capacities are then in series with the semiconductor space charge region ( $C_R$ ). This relationship can be expressed as follows:

$$\frac{1}{C_T} = \frac{1}{C_H} + \frac{1}{C_G} + \frac{1}{C_R} \quad (\text{Eq. 11})$$

In moderately concentrated electrolytes, the diffuse double layer is suppressed, and  $C_G$  can be neglected. In metals,  $C_H$  is approximately  $20\text{-}100 \frac{\mu\text{f}}{\text{cm}^2}$ , which is much larger than  $C_T$  measured for semiconductors; therefore,  $C_T$  measured is almost equal to the space charge capacity of a semiconductor.  $U_R$  is not directly measurable but has been shown to be related to the potential measured ( $U_E$ ) and to the potential across the Helmholtz layer ( $U_H$ ) in the following manner (?):

$$U_E = U_R + U_H + \text{constant} \quad (\text{Eq. 12})$$

When  $C_T$  is plotted versus  $U_E$ , a minimum is observed as illustrated in Figure 15. It can be shown (8, p. 60) that for an intrinsic semiconductor this minimum corresponds to the potential at which there is no potential drop across the space charge region; that is, the minimum corresponds to the flat-band potential. For an n-type semiconductor the potential minimum is more positive than the flat-band potential while that of a p-type is more negative (8, p. 60).

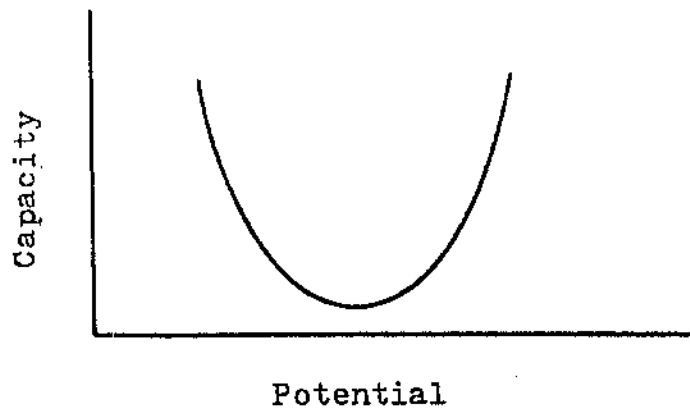


Fig. 15--Space charge capacity as a function of potential.

Dewald (3, p. 619) has derived the following expression to describe the relationship between capacity and potential upon anodic polarization for an n-type semiconductor with a large band gap (in specific for ZnO):

$$C_R = \left( \frac{q^2 N_D a b}{2KT} \right)^{\frac{1}{2}} (-f + \ln f - U_E)^{-\frac{1}{2}} \quad (\text{Eq. 13})$$

where  $N_D$  is the donor density,  $q$  is the electronic charge,  $a$  is the dielectric constant for ZnO,  $b$  is the permittivity of vacuum,  $f$  is the fraction of donors that are ionized in the bulk of the semiconductor, and the other terms have their usual significance. A plot of  $U_E$  versus  $\left( \frac{1}{C_R} \right)^2$  gives a straight line whose slope can be used to determine the donor density. An extrapolation of the linear portion of the  $U_E$  versus  $\left( \frac{1}{C_R} \right)^2$  plot to the voltage axis gives the potential

at which the flat-band potential has been bent up by a factor of  $\frac{kT}{q}$ . For example Lohmann (7, p. 430) has used this method to determine the flat-band potential for ZnO as a function of pH and has found that the flat-band potential changes linearly with pH at the rate of 54 millivolts per pH unit.

One result of the semiconductor space charge layer is that the potential distribution is more complicated for a semiconductor than for a metal. In a metal there is no space charge region; consequently, most of the potential drop occurs in the solution part of the double layer; in a semiconductor large potential drops can occur in the space charge region as well as in the solution part of the double layer. The potential distribution for a semiconductor can be illustrated as shown in Figure 16. Another complication arises in the differences involved in the transfer of charge carriers at the solid-solution interface. For metals, reactions at the solid-solution interface involve only electrons from the conduction band. The processes occurring at the semiconductor-solution interface are more complicated because these processes can involve electrons from the conduction band, holes from the valence band, or a mixture of both holes from the valence band and electrons from the conduction band.

When the half-cell reactions at a semiconductor-solution interface involve both holes from the valence

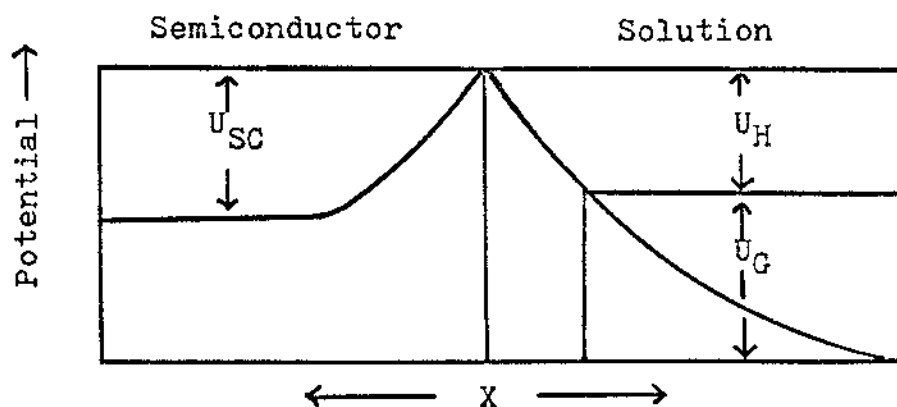


Fig. 16--Potential distribution around a semiconductor-solution interface: ( $X$ ) distance from surface, ( $U_{SC}$ ) potential drop across the semiconductor space charge region, ( $U_H$ ) potential drop across the Helmholtz layer, ( $U_G$ ) potential drop across the Gouy layer.

band and electrons from the conduction band, the semiconductor exhibits a photovoltaic effect upon irradiation with light. N-type semiconductors show a shift in the open circuit potential to more cathodic values when irradiated with the proper energy light; p-type semiconductors show a shift in the open circuit potential to more anodic values. For an n-type semiconductor (a similar reasoning also holds for the p-type) this effect is a result of the presence of many more electrons in the conduction band than holes in the valence band and also of the existence of the mixed potential that occurs at open circuit. The two half-cell reactions are illustrated in Figure 17. Curves A and B represent the two half-cell reactions in the dark, and

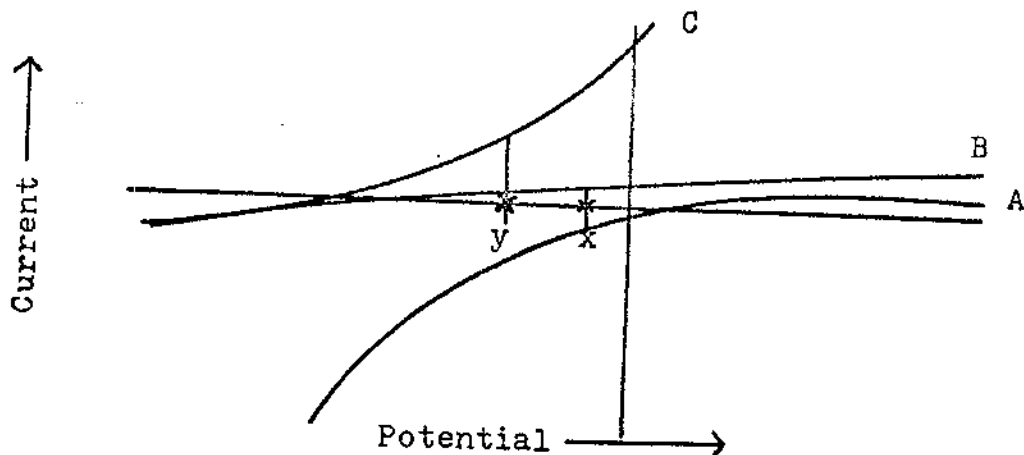


Fig. 17--Representation of mixed potential ( $U_M$ ) on ZnO in an alkaline solution: (x) open circuit potential in the dark, (y) open circuit potential in light, (A and B) half cell reactions in dark, (C) anodic half cell reaction in light.

point x represents their open circuit potential. When the semiconductor is irradiated with the proper energy light, holes are generated in the valence band, and electrons are delocalized into the conduction band; however, there are already many electrons in the conduction band; therefore, the addition of a few more does not appreciably increase or alter the lower curve (hydrogen gas curve). However, there are few holes present in the dark; consequently, the generation of additional holes greatly affects the half-cell reaction that depends upon holes. Assuming this is curve B, this rate will be increased, say to curve C. Since one of the half-cell reactions has been increased, the other one must be altered if the open circuit condition of no net current is to be maintained. This equal and opposite current

condition is now met in Figure 17 by point y which is a more cathodic open circuit potential. This effect was observed in the present study with ZnO by connecting a high intensity microscope lamp into a variable transformer and then increasing the voltage to the lamp. As the voltage was increased, the intensity of the lamp was increased, and thus the number of electron-hole pairs generated was increased. As the number of holes was increased, the open circuit potential increased in a cathodic direction, as shown in Figure 18.

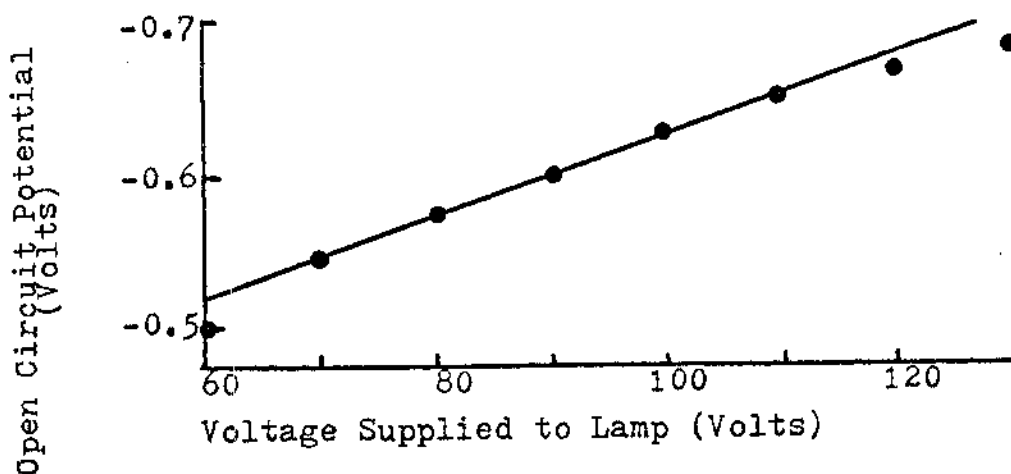


Fig. 18--Open circuit potential of ZnO in 1N KOH as a function of relative light intensity.

Due to differences in bulk properties of metals and semiconductors, the kinetic expression for describing an electrochemical reaction at a semiconductor-solution interface is more complicated than that for a metal-solution interface. The general relation between current

and potential for the majority carrier can be expressed as follows:

$$i = i_n^0 \left[ e^{\frac{F}{RT} (-\alpha\eta + \epsilon_1 - \epsilon_1^0)} - e^{\frac{(1-\alpha)F\eta}{RT}} \right] + i_p^0 \left[ e^{-\frac{\alpha F \eta}{RT}} - e^{\frac{F}{RT} \{ (1-\alpha)\eta - \epsilon_1 + \epsilon_1^0 \}} \right] \quad (\text{Eq. 14})$$

where  $i$  is the net current,  $i_n^0$  is the current due to the flow of electrons,  $\eta$  is the potential drop in the Helmholtz layer,  $\epsilon_1 - \epsilon_1^0$  is the potential drop across the semiconductor space charge region,  $i_p^0$  is the current due to the flow of holes, and the other terms have their usual significance.

If the hole current is much smaller than the electron current (as in the cathodic polarization of an n-type semiconductor), then the contribution by the valence band to the net current can be neglected, or the contribution of the conduction band to the net current can be neglected upon anodic polarization of a p-type semiconductor. Using an n-type semiconductor as an example, the current-voltage relationship can be simplified to the following expression:

$$i = i_n^0 \left[ e^{\frac{F}{RT} (-\alpha\eta + \epsilon_1 - \epsilon_1^0)} - e^{\frac{(1-\alpha)F\eta}{RT}} \right] \quad (\text{Eq. 15})$$

Two limiting cases can be examined. If the potential drop in the Helmholtz layer is much greater

than that in the semiconductor space charge region, the expression simplifies to

$$i = i_n^0 \left[ e^{\frac{-\alpha F \eta}{RT}} - e^{\frac{(1-\alpha) F \eta}{RT}} \right] \quad (\text{Eq. 16})$$

which is the Tafel expression for metals. If the potential drop in the space charge region is much larger than that in the Helmholtz layer (a more likely situation for semiconductors), equation 15 becomes

$$i = i_n^0 \left[ e^{\frac{F}{RT} (\epsilon_1 - \epsilon_1^0)} - 1 \right] \quad (\text{Eq. 17})$$

When the logarithm of both sides is taken, the following relation is obtained:

$$\ln i = \ln i_n^0 + \frac{F}{RT} (\epsilon_1 - \epsilon_1^0) \quad (\text{Eq. 18})$$

Thus a plot of  $\ln i$  versus  $(\epsilon_1 - \epsilon_1^0)$  gives a straight line whose slope is approximately the same value as that obtained from the Tafel plot for metals. A similar "Tafel-like" relation is found for the anodic polarization of p-type semiconductors.

These two cases indicate that under cathodic polarization of n-type semiconductors and anodic polarization of p-type semiconductors there is an ample supply of charge carriers at the surface of the semiconductor and that the slow step in the overall reaction is the charge transfer step and not a diffusion of



charges to the semiconductor surface from the bulk of the semiconductor. Under these conditions the semiconductor acts much like a metal.

When the density of charge carriers is small, as in the anodic polarization of an n-type semiconductor or the cathodic polarization of a p-type semiconductor, the overall rate may not be controlled by charge transfer but by diffusion of charge carriers to the surface from the semiconductor bulk. In this type of reaction the current increases to a limiting value and then remains approximately constant.

The anodic polarization of n-type semiconductors has been studied more than the cathodic polarization of p-type material. In a classical work Brattain and Garrett obtained the following expression for the anodic polarization of n-type germanium (2):

$$\epsilon_1 = \epsilon_1^{\circ} + \frac{qRT}{KTF} \ln \frac{|i|}{i_0} - \frac{RT}{F} \ln \left( 1 - \frac{i}{i_{lim}} \right) + IR \quad (\text{Eq. 19})$$

where  $i_{lim}$  is the limiting current which is normally associated with the diffusion of holes in the space charge region,  $q$  is again the electronic charge, and the other terms have their usual significance.

If the supply of holes is large enough (as in the case for germanium which has a relatively small band gap energy), the last two terms can be neglected for

values of the net current much smaller than the limiting current. Under these conditions the following "Tafel-like" relation is found:

$$\epsilon_1 - \epsilon_1^0 = \frac{qRT}{kTF} \ln \frac{|i|}{i_0} \quad (\text{Eq. 20})$$

Equation 20 has the same form as the following Boltzmann equation for a large distribution of holes:

$$p_s = p_0 e^{\frac{-q(\epsilon_1 - \epsilon_1^0)}{kT}} \quad (\text{Eq. 21})$$

where  $p_s$  is the hole density at the surface, and  $p_0$  is the hole density in the bulk. For an n-type semiconductor under anodic polarization, these two expressions can be shown to be related (8, p. 19); therefore, the current for this case is directly related to the arrival of holes at the surface.

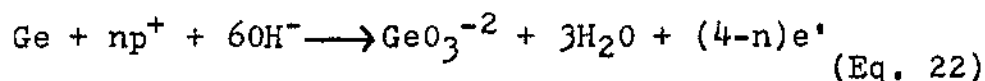
For n-type semiconductors with large band gaps, such as ZnO, the hole density is small; therefore, upon anodic polarization the current very quickly approaches the limiting current, and a Boltzmann equation is not applicable. Under these conditions the last terms in equation 19 become important as the rate determining step in the overall reaction. Depending upon the careful control of external parameters, such as the wavelength of incident light and the presence of oxygen, current-voltage relationships for large band gap semiconductors may or may not obey the Tafel relation and

also may or may not exhibit a clear cut limiting current. When these parameters are carefully controlled, reproducible polarization curves with regions in which certain electrochemical reactions at the electrode surface can be observed and measured are obtainable as were found in the present study with ZnO. Because the system becomes more difficult to study as the band gap increases, it is very difficult to analyze the reactions occurring during the dissolution of a wide band gap semiconductor like ZnO; nevertheless, capacities, polarization data, and photoeffects can be used to postulate and verify some of the electrochemical reactions at the semiconductor surface. With the conclusion of the present study with ZnO, corrosion data and its electrochemical sensitivity will be added to what has already been done thus far by others, limited though it has been.

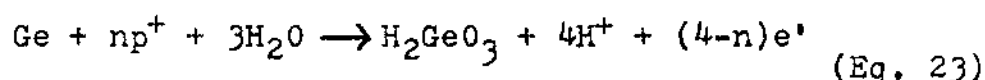
Of the semiconductors studied, the dissolution mechanisms for germanium and silicon have been the most well-established. The polarization data of Brattain and Garrett (2) for n-type germanium exhibited a saturation current upon anodic polarization; this saturation current was increased by irradiating the germanium electrode with light and also by injecting holes from the reverse side of a thin germanium slice. These data can be interpreted as evidence that the anodic reaction depends upon the availability of holes

at the surface. Beck and Gerischer (1) proposed the following mechanism for the anodic dissolution of germanium:

(a) In alkaline solution



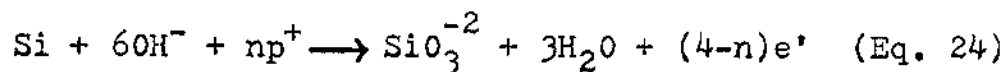
(b) In acidic solution



where  $n$  is a constant (usually 2.4),  $\text{p}^+$  is a hole, and  $\text{e}'$  is an electron. In open circuit corrosion these half-cell reactions are accompanied by hydrogen evolution as in metals.

As the width of the band gap increases from 0.66 eV for germanium to 1.09 eV for silicon, the dissolution processes become more difficult to formulate. Silicon dissolution processes are additionally complicated by oxide layers that are measurably soluble only in alkaline or HF solutions. Izidinov (6) has found that in 10 N KOH silicon dissolves essentially by a chemical mechanism; however, Hurd and Wrotenbery (5) have clearly shown that in less basic solutions (approximately 1 N KOH) the dissolution rates of silicon are potential dependent and in fact parallel polarization data as shown in Figure 19 for an n-type silicon crystal. The potential dependency indicates that the silicon dissolution rate is at least partially electrochemical in

nature. The importance of the hole supply for the dissolution process was illustrated by comparisons of polarization curves for p and n-type crystals. The current density at the onset of passivity (a phenomenon in which a film develops on the electrode surface and reduces the rate of electrochemical dissolution) was shown to be significantly higher for p-type material; the potentials throughout the rising part of the passive peak (the potential on a potential-current curve at which the anodic current decreases as the result of a protective film formation) also were more positive for the p-type. When n-type samples were irradiated, the anodic current increased by about an order of magnitude; the capacity in aqueous HF under anodic polarization also increased under illumination. These data were used to formulate the following anodic half-cell reaction for silicon dissolution in alkaline solutions:



In open circuit corrosion this half-cell reaction is again accompanied by hydrogen evolution as in metals and germanium.

ZnO has an even wider band gap (3.2 eV) than germanium and silicon. Most of the previous work concerning the ZnO-solution interface has been based upon capacity measurements. For example Hauffe (4) found that the

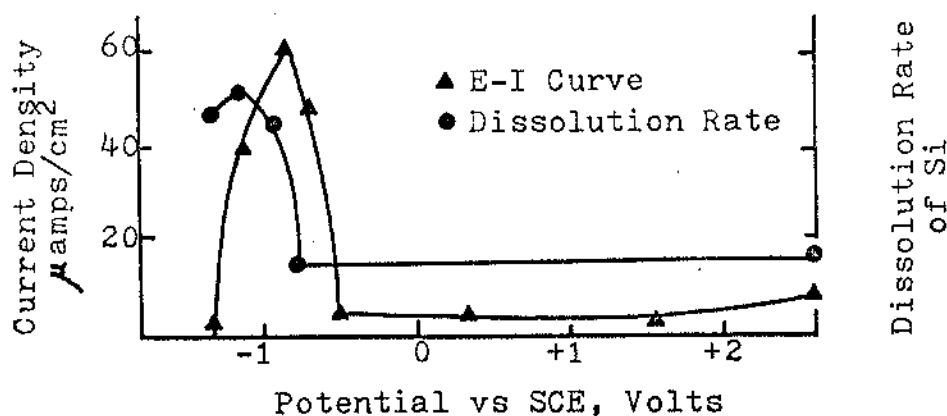


Fig. 19--Correlation of silicon dissolution rate with current-voltage relation (5, p. 893).

capacity minimum shifted to more cathodic values with increasing pH values. In addition, plots of  $\frac{1}{C^2}$  versus potential for ZnO electrodes both in the dark and in light indicated that the flat-band potential changed only very slightly upon irradiation. Hauffe interpreted the large open circuit potential shift observed upon irradiation (the measured photovoltage) as being due to the displacement of voltage in the space charge layer of the ZnO crystal. His data also showed that the anodic current increased upon illumination. None of the previous work established the nature of the dissolution processes occurring at the ZnO-solution interface. As a step toward understanding these processes, the objective of this research program was to determine whether or not the dissolution rates of single crystal ZnO were potential dependent, that is, whether or not an electrochemical mechanism, in analogy to metals and

elemental semiconductors, governs all or part of the dissolution process. In order to study the processes occurring at a ZnO electrode, it is necessary to understand the structure of ZnO single crystals and the causes of semiconduction in these crystals. In the following chapter these specific properties of ZnO are discussed along with a brief summary of previous work with ZnO.

## CHAPTER BIBLIOGRAPHY

1. Beck, F. and Gerischer, H., "Zum Mechanismus der Anodischen Auflösung von Germanium in Alkalischer Lösung," Zeitschrift für Elektrochemie, LXIII (April, 1959), 500-510.
2. Brattain, W. and Garrett, C., "The Interface Between Germanium and an Electrolyte," The Bell System Technical Journal, XXXIV (January, 1955), 129-177.
3. Dewald, J. F., "Charge and Potential Distribution at the Zinc Oxide Electrode," The Bell System Technical Journal, XXXIX (May, 1960), 615-639.
4. Hauffe, Von K. and Range, J., "Über die anodische Auflösung von Zinkoxid-Einkristallen unter Lichteinwirkung," Berichte der Bunsengesellschaft, LXXI (July, 1967), 690-697.
5. Hurd, R. M. and Wrotenbery, P. T., "Electrochemistry of the Silicon-Electrolyte Interface," Annals of the New York Academy of Science, CI (January, 1963), 876-903.
6. Izidinou, S. U. and others, "Electrochemical and Photoelectrochemical Behavior of the Silicon Electrode," Doklady Akademii Nauk SSSR, CXXXIII (July, 1960), 392-395.
7. Lohmann, F., "Der Einfluss des pH auf die Elektrischen und Chemischen Eigenschaften von Zinkoxidelektroden," Berichte der Bunsengesellschaft, LXX (April, 1966), 428-434.
8. Myamlin, V. A. and Pleskou, Y. V., Electrochemistry of Semiconductors, New York, Plenum Press, 1967.



## CHAPTER III

### PREVIOUS EXPERIENCE IN ELECTROCHEMISTRY AND DISSOLUTION OF ZnO

For many years powdered ZnO has been used extensively in industry. As examples, powdered ZnO is widely used in paints, cosmetics, rubber products, ceramic products, and so on. This powdered ZnO probably dissolves by a chemical mechanism. Blok (1, p. 29) has found a minimum of solubility for powdered ZnO in the pH range from about nine to twelve; Parks (10) has shown that this corresponds to a zero point of charge; that is, this range encompasses pH values at which there is relatively little specific adsorption of potential determining ions ( $H^+$  or  $OH^-$ ) on the ZnO surface.

In addition to powdered ZnO, single crystals are now available. Due to their much smaller surface area per volume ratios and to their different bulk properties, these crystals may dissolve by a completely different mechanism. Dewald (3), Hauffe (5), Blok (1), and Lohmann (6) have used capacity measurements to investigate the ZnO (single crystal)-electrolyte interface under a variety of external conditions. Morrison and Freund (9) have used single crystal ZnO electrodes in the photocatalysis of certain organic molecules. In a recent

paper Williams (12) has found under certain experimental conditions that the charge determined by measuring the current in the external circuit for a ZnO single crystal electrode was essentially equal to the charge carried into solution by donors as determined from capacity and volume measurements. In a general paper concerning the behavior of semiconductors under illumination, Gerischer (4) has discussed the decomposition of a single crystal ZnO electrode under illumination. None of these authors, however, has measured the dissolution rates of a single crystal of ZnO, nor have they suggested that these rates may be potential dependent.

Single crystals of ZnO are n-type semiconducting crystals with a wide forbidden gap (3.2 eV). Their usual method of preparation is that of Scharowsky (11), for which the apparatus is illustrated in Figure 20.

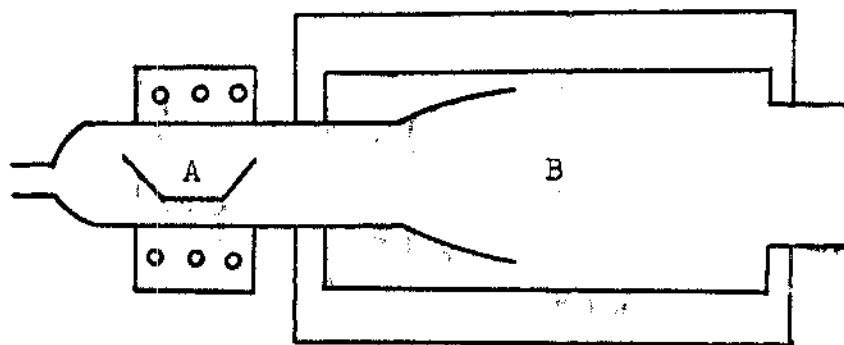


Fig. 20--Apparatus for producing ZnO single crystals: (A and B) furnace chambers.

Zinc metal is placed in unit A and heated to about  $600^{\circ}\text{C}$ . A stream of nitrogen containing about 1 per cent hydrogen is passed over the metal and is used to carry the zinc vapor from chamber A to furnace chamber B. In furnace B the zinc vapor is heated in the presence of air to  $1150^{\circ}\text{C}$ . Single crystals up to ten centimeters in length and one centimeter in diameter have been reported (2, p. 28) to form on the edge of the funnel shaped entrance tube between furnaces A and B; however, the most common lengths and widths are between two and fifteen millimeters and between one and five millimeters, respectively; the larger diameter crystals are much shorter in length.

The large band gap of  $\text{ZnO}$  prevents the observance of intrinsic semiconductance. All single crystals exhibit n-type semiconductance which probably arises from the presence of interstitial zinc trapped in the crystal during its growth. Mohanty and Azaroff (8) have determined electron distributions in single crystal  $\text{ZnO}$  by measurement of x-ray diffraction intensities. Their data have indicated large numbers of interstitial zinc atoms in  $\text{ZnO}$ ; the density of interstitial zinc was about one thousand times greater than the values for the donor density calculated from electrical conductivities; this discrepancy was interpreted as being due to most of the interstitial zinc atoms being electrically neutral.

The valence electrons in zinc and oxygen are believed to be in  $sp^3$  hybrid orbitals, and the atoms are held together in a tetrahedral structure. The crystal forms in layers along the longitudinal axis (c-axis) as shown in Figure 21. In Figure 21 it can be seen that there are three bonds between each zinc atom and layer 1 but only one bond between each zinc atom and layer 3. When pressure is applied perpendicular to the c-axis, there is a higher probability that the crystal will break perpendicular to this axis and between layers 2 and 3 rather than 2 and 1.

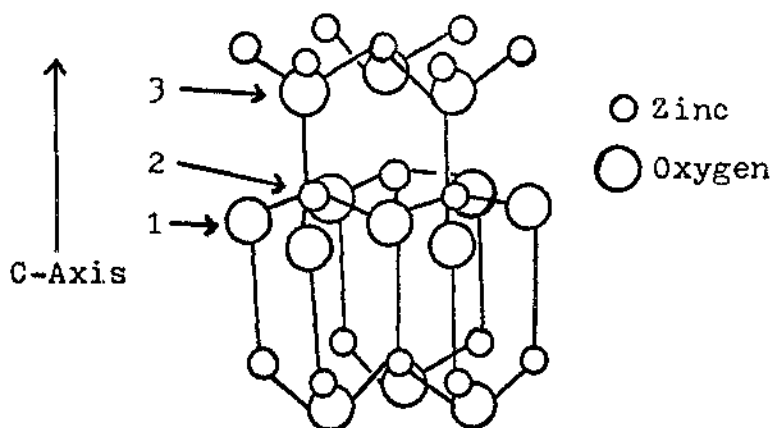


Fig. 21--Representation of crystal lattice of ZnO (6); (1) and (3) oxygen layers, (2) zinc layer.

The splitting exposes a zinc face (the  $\langle 0001 \rangle$  face) and an oxygen face (the  $\langle 000\bar{1} \rangle$  face). If the oxygen (or zinc) face were originally exposed, then an oxygen (or zinc) face is again exposed during polishing operations so that the final polished face is the same

type as the original. This statement is not meant to imply that the polished face is a completely smooth surface of either oxygen or zinc atoms. There probably are steps in the surface as shown in Figure 22; however, it is believed that all the horizontal portions of the steps have a high probability of exposing either essentially zinc or oxygen atoms.

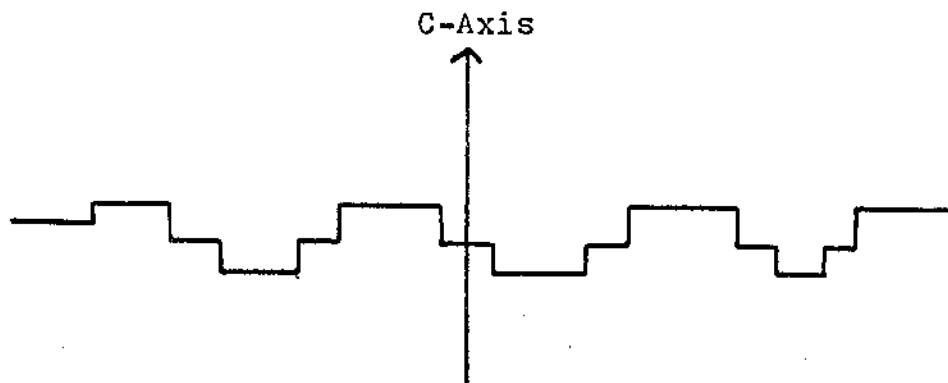


Fig. 22--Profile of a ZnO surface

Zinc and oxygen atoms in ZnO share two covalent bonds; in addition, each oxygen atom supplies two co-ordinate covalent bonds; however, all four bonds are in resonance (7). Oxygen is significantly more electro-negative than zinc (3.5 for oxygen and 1.5 for zinc); consequently, there is some partial ionic bond character present in which the oxygen atoms increase their electron density by attracting bonding electrons at the expense of zinc atoms. When the crystal is split, each atom of an exposed oxygen layer has a high probability of possessing a dangling pair of electrons at the surface.

Each atom of the exposed zinc layer has a high probability of having an empty orbital which is in addition to the decreased electron density around the zinc atom; therefore, atoms of the exposed zinc face can be pictured as having a partial positive charge and those of the exposed oxygen face as having a partial negative charge. The dissolution rates on the two faces are different; therefore, it is necessary to use one face throughout a study; in the present study with ZnO the zinc face was used because it exhibited slow, uniform dissolution across the surface in KOH and rapid, irregular dissolution in  $H_2SO_4$ . The oxygen face would be expected to be etched faster by electrophilic substances ( $HNO_3$ ) than the zinc face. Oxygen and zinc faces have been identified by x-ray data (?); when placed in  $HNO_3$  the identified oxygen face was indeed quickly pitted whereas the zinc face under the same conditions was not noticeably changed. The effect was so dramatic that etching properties can be used as an experimental tool to identify the exposed face.

## CHAPTER BIBLIOGRAPHY

1. Blok, L., The Ionic Double Layer on Zinc Oxide in Aqueous Electrolyte Solutions, "Bronder-Offset" Rotterdam, 1968.
2. Brown, H. E., Zinc Oxide Rediscovered, New York, The New Jersey Zinc Company, 1957.
3. Dewald, J. F., "Charge and Potential Distribution at the Zinc Oxide Electrode," The Bell System Technical Journal, XXXIX (May, 1960), 615-639.
4. Gerischer, H., "Electrochemical Behavior of Semiconductors under Illumination," Journal of the Electrochemical Society, CXIII (November, 1966), 1174-1180.
5. Hauffe, Von K. and Range, J., "Uber die anodische Auflosung von Zinkoxid-Einkristallen unter Lichteinwirkung," Berichte der Bunsengesellschaft, LXXI (July, 1967), 690-697.
6. Lohmann, F., "Der Einfluss des pH auf die Elektrischen and Chemischen Eigenschaften von Zinkoxidelektroden," Berichte der Bunsengesellschaft, LXX (April, 1966), 428-434.
7. Mariano, A. N. and Hanneman, R. E., "Crystallographic Polarity of ZnO Crystals," Journal of Applied Physics, XXXIV (February, 1963), 384-388.
8. Mohanty, G. P. and Azaroff, L. V., "Electron Density Distributions in ZnO Crystals," The Journal of Chemical Physics, XXXV (October, 1961), 1268-1270.
9. Morrison, S. R. and Freund, T., "Chemical Role of Holes and Electrons in ZnO Photocatalysis," The Journal of Chemical Physics, VLII (August, 1967), 1543-1551.
10. Parks, G. A. and de Bruyn, P. L., "The Zero Point of Charge of Oxides," Journal of Physical Chemistry, LXVI (October, 1962), 967-973.

11. Scharowsky, E., "Optische und elektrische Eigenschaften von ZnO-Einkristallen mit Zn-Uberschuss," Zeitschrift fur Physik, CXXXV (June, 1953), 318-330.
12. Williams, R., "Electrical Effects of the Dissolution of n-Type Zinc Oxide," Journal of Applied Physics, XXXIX (August, 1968), 4089-4091.



## CHAPTER IV

### EXPERIMENTAL

Zinc oxide single crystals were obtained from Electronic Space Products, Inc. The physical dimensions, resistivity values, and conductivity values for the crystals used in this study are shown in Table 1. According to emission spectroscopy analyses furnished by Electronic Space Products, Inc., the maximum impurity level for the raw ZnO crystals was fifty-five parts per million impurities, other than zinc.

TABLE I  
PHYSICAL PROPERTIES AND DIMENSIONS  
OF ZnO SINGLE CRYSTALS

Crystal #	Length (mm)	Area (cm <sup>2</sup> )	Resistivity (ohm-cm)	Conductivity (ohm-cm) <sup>-1</sup>
1	11	0.026	6.1	0.16
2	12	0.042	10.0	0.10
3	12	0.041	8.5	0.12
4	11	0.040	4.4	0.23
5	12	0.038	2.0	0.50

In order to obtain resistivity and conductivity values and also to be able to use the hexagonal ZnO crystals as electrodes, "ohmic" contacts (so-called because the relation between the current and the potential

drop at the contact obeys Ohm's law (2, p. 144)) had to be secured to the tips of the crystals. Ohmic contacts were obtained to the ZnO single crystals by a method used by Dewald (1). Onto a tip of the crystal a layer of indium was electroplated at a current density of about two milliamperes per  $\text{cm}^2$  from 100 milliliters of solution containing two grams of indium sulfate and one gram of sodium sulfate. On top of the indium, a copper layer was electroplated again at a current density of about two milliamperes per  $\text{cm}^2$  from 100 milliliters of a solution containing 2.2 grams of  $\text{Cu}_2(\text{CN})_2$ , 3.4 grams of NaCN, and 1.5 grams of  $\text{Na}_2\text{CO}_3$ . About one hour was required to electroplate a uniform layer of indium and about four hours were required for copper. By heating the copper and indium plated tip, solder was applied to the electroplated area. While still maintaining the solder in a molten state, a heated copper wire was placed in the molten solder. Upon cooling a strong contact was formed, as shown in Figure 23; the strength of the contact could be tested by simply trying to pull the copper wire away from the crystal. Even with strong pulling the wire could not be separated from the crystal.

In order to determine the resistivities of the crystals, ohmic contacts were obtained to both ends of the crystals, and the resistance was measured with a Gray Instrument Company Wheatstone bridge. When the



Fig. 23--Electrical contact to ZnO single crystal (approximately 40 magnification).

leads from the Wheatstone bridge to the crystal were reversed, the same resistance was obtained; also when a variable voltage was applied to the crystal and the current in the circuit measured, an Ohm's law relationship was obtained. Thus the contacts were shown to have been ohmic.

Surface areas and lengths were obtained under 45 magnification by the use of an American Optical microscope. The microscope base was set in a mobile stage that could be moved "right and left" with respect to the operator by a calibrated turning knob. The distance moved was divided in units of 0.025 inches. These units were subdivided by a 0.000 to 0.025 inch vernier scale which was divided in units of 0.001 inches. The ten-thousandth place value could be estimated. This "right

and left" base was set in another mobile stage that could be moved "to and from" the operator by another similarly calibrated turning knob. A hair was firmly attached to the lens of the microscope and used as a pointer. The hexagonal surface was "divided" into four triangles as shown in Figure 24; the areas were determined by the following expressions:

$$2S = a + b + c \quad (\text{Eq. 25})$$

$$\text{Area} = \sqrt{(S)(S-a)(S-b)(S-c)} \quad (\text{Eq. 26})$$

where a, b, and c are the lengths of the three sides of a triangle.

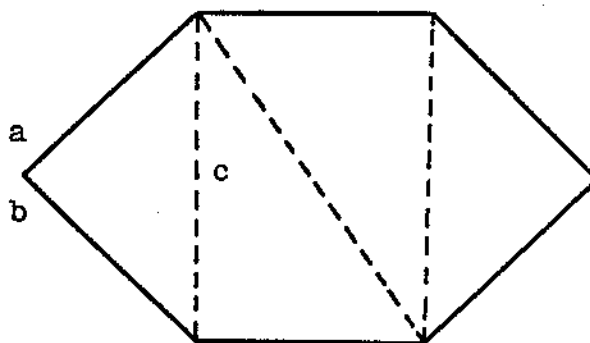


Fig. 24--Representation of ZnO face (perpendicular to c-axis).

The crystals were split perpendicular to the c-axis (the longitudinal axis) by applying pressure with a razor blade. As discussed in Chapter III this exposed one face which had a high surface density of oxygen atoms (the  $\langle 000\bar{1} \rangle$  face) while the opposite face had a

high surface density of zinc atoms (the  $\langle 0001 \rangle$  face). When the zinc face was placed in 20 per cent nitric acid for thirty seconds, no change was observed on the surface; when the oxygen face was placed in the same 20 per cent nitric acid solution for thirty seconds, the surface was covered with small etch pits which could be seen with the naked eye and clearly distinguished with the aid of a microscope. Smooth surfaces were obtained by placing jeweler's rouge and 0.3 micron abrasive spray on 0.05 to 0.25 micron alumina polishing discs and then polishing the crystal against the disc until the exposed surface appeared smooth under 45 magnification. As discussed in Chapter III the zinc face was continually exposed during the polishing; therefore, the final polished face was still the zinc face.

The copper lead was placed through a glass rod, and the sides of the crystal, contact, and glass rod were coated with "Liquid Tape" from G. C. Electronics Company. The cells used for the electrochemical measurements are represented in Figure 25.

The circuit for measuring polarization curves and also for maintaining a constant potential was a standard three electrode system as shown in Figure 26.

Corrosion rates were determined by measuring the accumulations of zinc ions in solution as a function of time. A Perkin-Elmer 303 Atomic Absorption Spectrophotometer was used for the zinc analysis. The

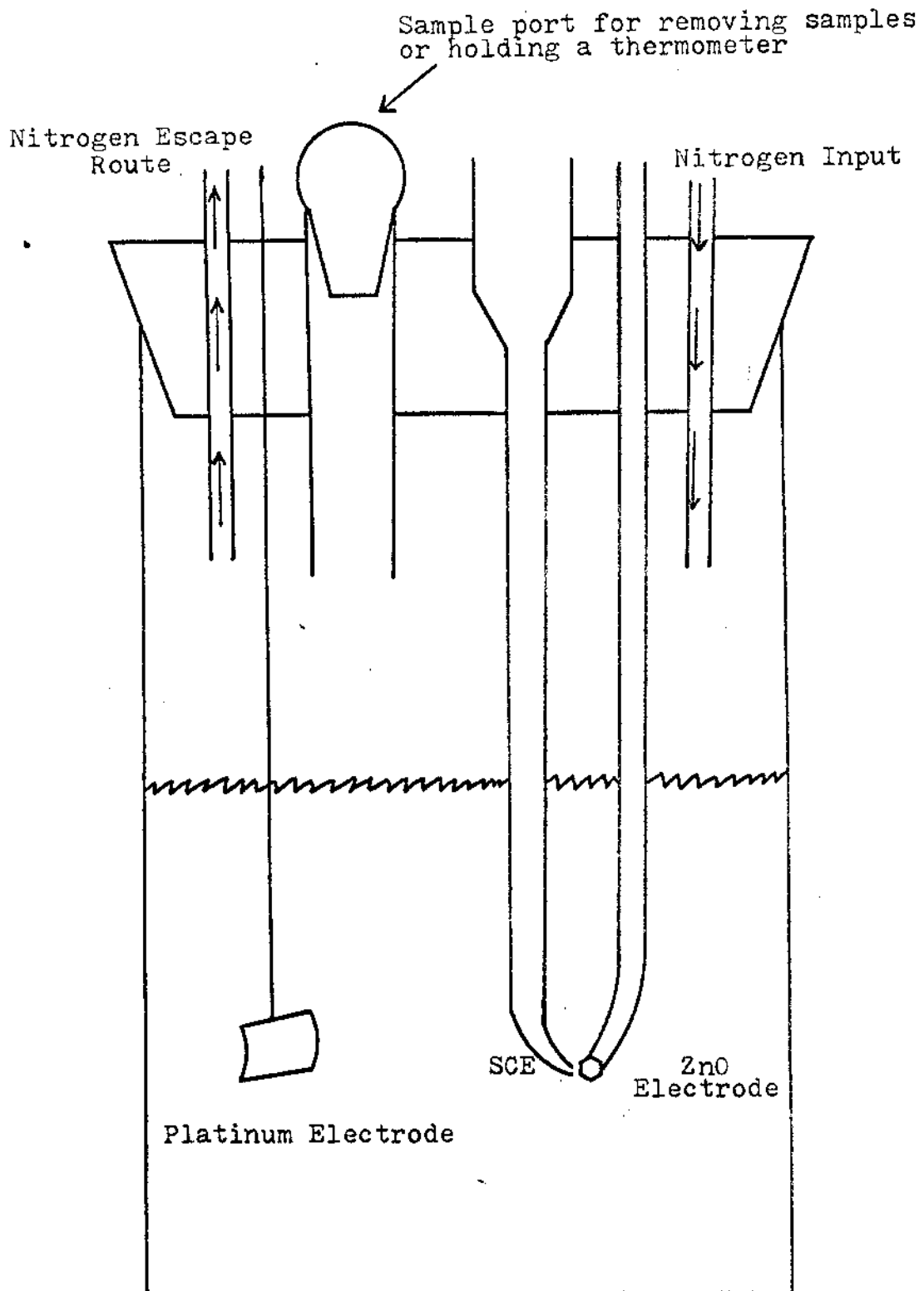


Fig. 25--Schematic diagram of electrochemical cell:  
(SCE) saturated calomel electrode.

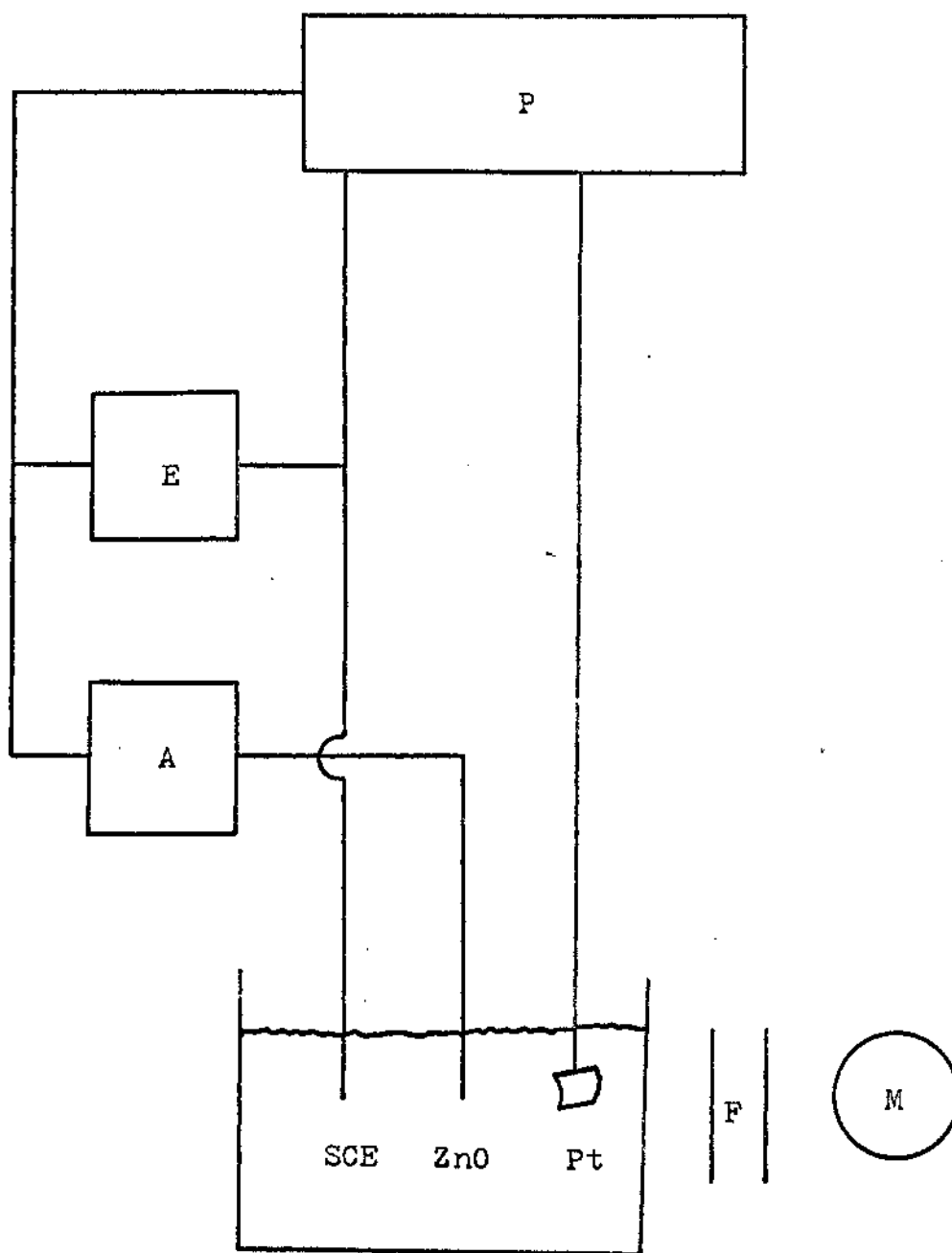


Fig. 26--Schematic diagram of circuit used to maintain a constant potential: (P) Magna "Anotrol" Model 4700m Potentiostat, (A) Keithley 410A Picoammeter, (E) Keithley 600A or 602 Electrometer, (SCE) saturated calomel electrode, (Pt) platinum electrode, (ZnO) ZnO electrode, (M) high intensity microscope lamp, (F) Corning light filter that filtered light above and below a 360 to 400  $m\mu$  band.

absorption line for zinc is approximately  $214 \text{ m}\mu$ ; at these wavelengths dust in the air and dust and films adsorbed on the instrument optics can scatter or absorb the emitted radiation; therefore, a great deal of care had to be exercised to keep the outside quartz windows of the spectrophotometer clean. The atomic absorption spectrophotometer was found to provide very accurate analyses from approximately 0.5 to about 3.00 parts per million; therefore, 0.75, 1.50, and 2.50 parts per million zinc solutions were used to prepare standard curves; when the same burner alignment and acetylene-compressed air flows were used, the standard curve changed very little over a 48 hour period. Preliminary data indicated that ZnO would dissolve in 50.00 ml of 1.0 N KOH at a rate of about 2.0 parts per million of zinc in about 40 hours; therefore, one set of standards could be used to measure each dissolution rate. The standards were prepared in either 1.0 N or 0.5 N KOH solutions in order to compensate for the 1.0 N or 0.5 N KOH experimental solvents. Three milliliter samples were found to be sufficient in volume for the zinc analyses; these test samples were removed by a 5.00 ml graduated pipette. A typical standardization curve is presented in Figure 27. The standardization curves were consistently very linear, and the concentration of zinc determined from these curves is believed to be accurate to the extent of  $\pm 0.03$  parts per million.



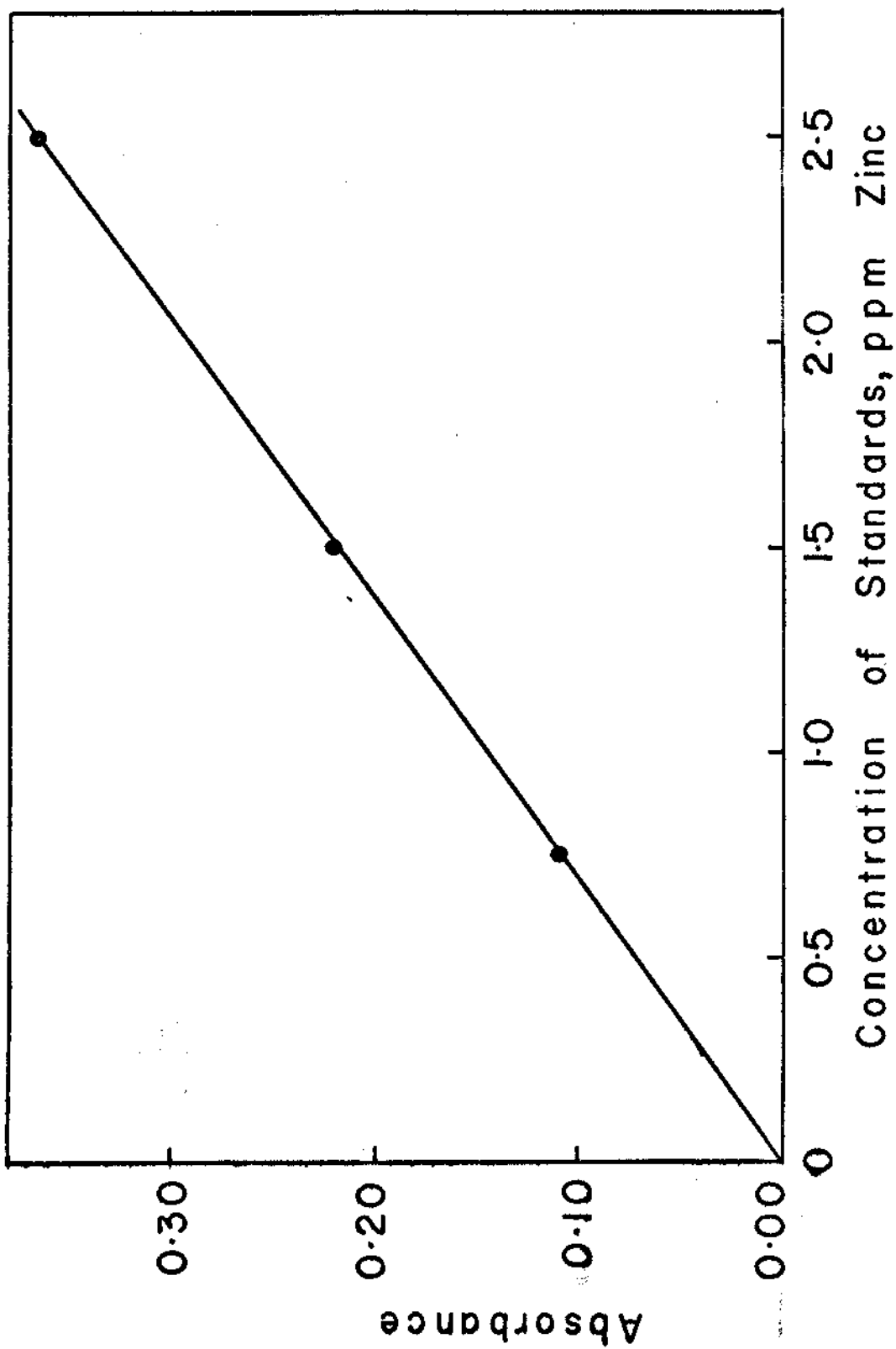


Fig. 27--Working curve relating absorbance to concentration for a routine zinc analysis by the atomic absorption method.

For the pH-potential relation, the pH was measured with a Coleman pH meter, and the potential was measured by a Keithley 600A or 602 Electrometer; the Coleman pH meter was used because the electrodes conveniently fit into the electrochemical cell. For potential-time studies, the potential was measured versus a saturated calomel electrode by a Keithley 600A or 602 Electrometer; output from the electrometer was recorded on a Brown recorder.

## CHAPTER BIBLIOGRAPHY

1. Dewald, J. F., "Charge and Potential Distribution at the Zinc Oxide Electrode," The Bell System Technical Journal, XXXIX (May, 1960), 615-639.
2. Myamlin, V. A. and Pleskou, Y. V., Electrochemistry of Semiconductors, New York, Plenum Press, 1967.

## CHAPTER V

### DATA

In order to determine a reference potential from which to begin each electrochemical measurement, a freshly polished zinc face of a carefully insulated ZnO single crystal was exposed to 1.0 N KOH solution; light was excluded from the electrochemical cell, and the potential was measured as a function of time. Immediately after immersion, the potential was approximately -600 millivolts versus a saturated calomel electrode (SCE), but then the open circuit potential (no imposed potential) drifted slowly with time toward more anodic potentials as shown in Figure 28. After about four hours, a reasonably stable open circuit potential of approximately -200 millivolts was obtained. When the crystal was removed from solution and allowed to remain under room conditions overnight, the potential immediately after immersion was approximately -150 millivolts versus SCE and drifted slowly to more cathodic values until again a reasonably stable open circuit potential of -200 millivolts was obtained. For all the remaining data, the polished crystals were placed in 1.0 N KOH for at least six hours before the actual experiment was begun. In all the experiments the dark open

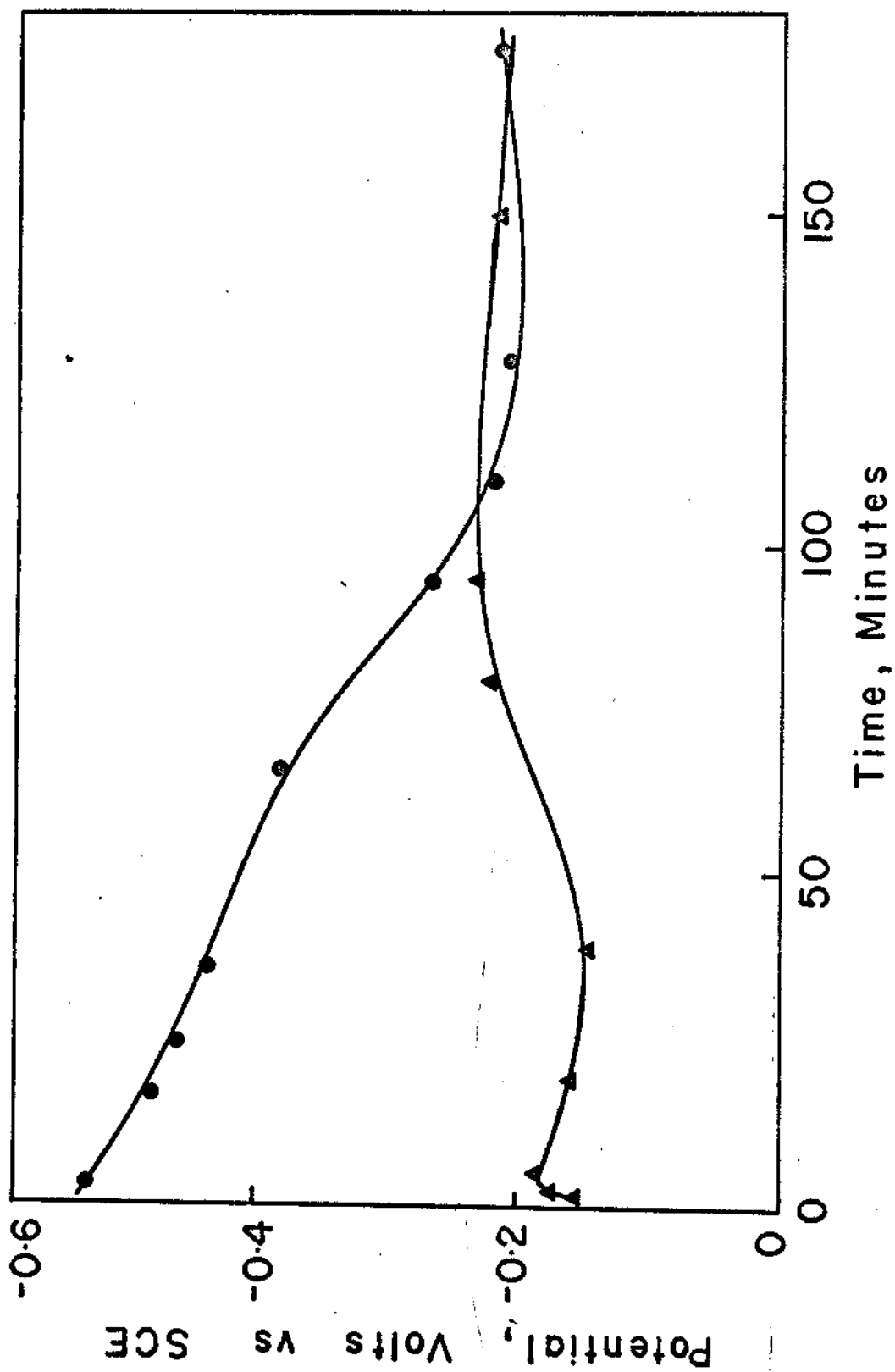


Fig. 28--(●) Change in potential of a freshly polished 2.0 ohm-cm ZnO single crystal in the dark in 1.0 N KOH. (▲) Change in potential for the crystal after it had been dissolved for six hours and then exposed to room conditions for twenty-four hours.

circuit potential was between -150 and -250 millivolts versus SCE.

The open circuit dissolution rate for the zinc face was then determined for an 8.5 ohm-centimeter single crystal in 1.0 N KOH. This rate was determined in the absence of light; oxygen was excluded from the electrochemical cell in this experiment and in all other work unless otherwise noted. Rates were then determined, likewise in the absence of light, at potentials three thousand millivolts anodic to SCE and twelve hundred millivolts cathodic to SCE. The three rates were determined from slopes of plots of milligrams of zinc accumulated in fifty milliliters of solution per  $\text{cm}^2$  of electrode surface versus time as shown in Figure 29. The values for these rates are also listed in Figure 29. Within experimental error, the dark rates were not affected by imposed potentials. This is shown more clearly in Figure 30, in which the dark dissolution rates are plotted as a function of potential on the same figure as a plot of current versus potential for the 8.5 ohm-centimeter crystal in 1.0 N KOH in the dark. Along the left hand ordinate is plotted the current in units of microamperes per square centimeter, while along the right hand ordinate is plotted the dissolution rate in units of milligrams of zinc in fifty milliliters of solution per  $\text{cm}^2$  per hour. For clarification, it should be pointed out that zero current density does not correspond to a zero dissolution rate. In all the correlation

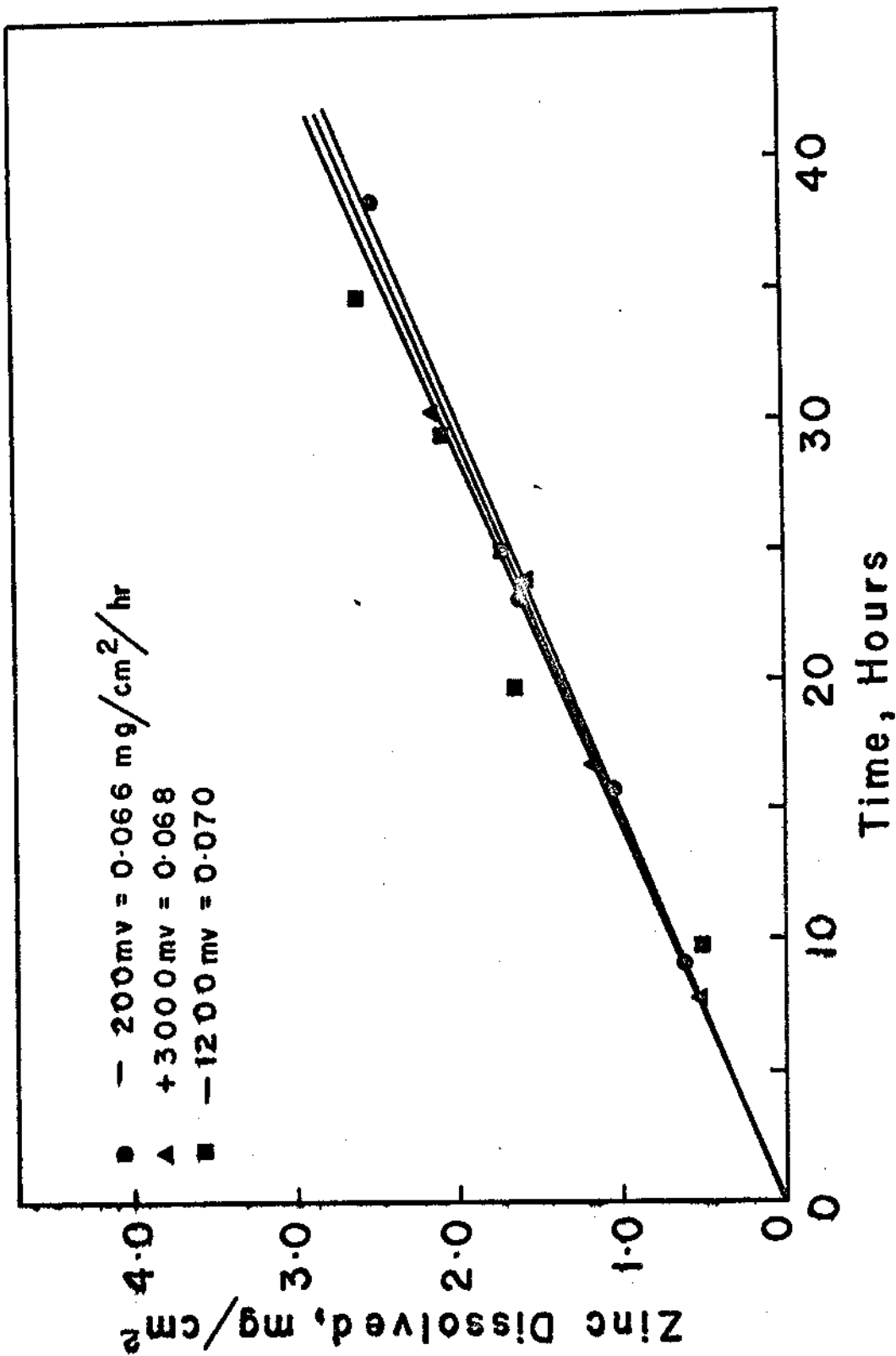
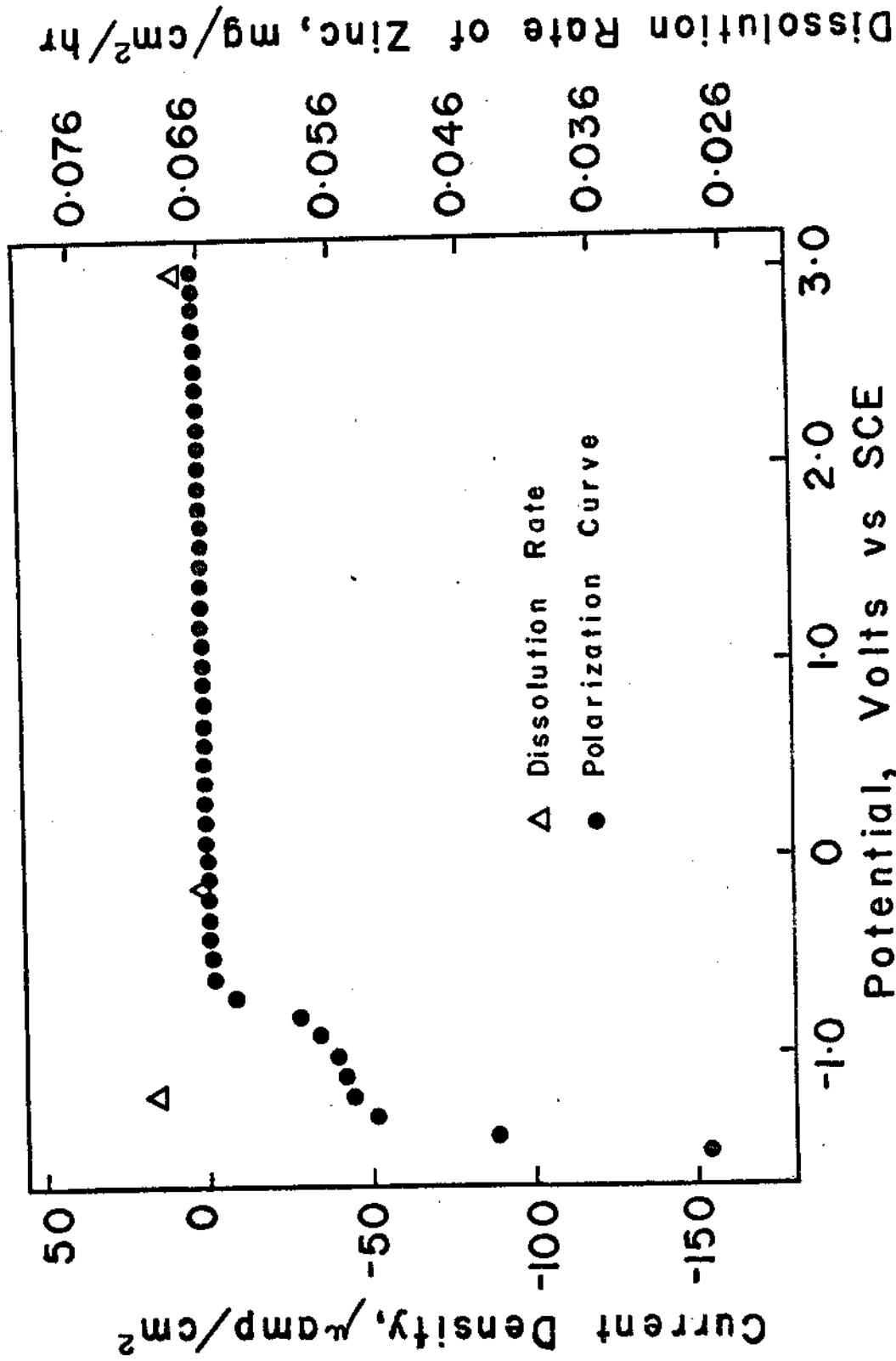


Fig. 29---Dissolution rates as a function of potential for the zinc face of an 8.5 ohm-cm ZnO single crystal in the dark in 1.0 N KOH at 31°C.



### Potential, Volts vs SCE

Fig. 30--Correlation of zinc dissolution rates with the current-voltage relation for the zinc face of an 8.5 ohm-cm ZnO single crystal in the dark in 1.0 N KOH at 31°C.



diagrams, the open circuit dissolution rate is plotted at zero current, and the anodic and cathodic dissolution rates are plotted with respect to this point.

Since the zinc dissolution rates in the absence of light were independent of potential, an attempt was made to increase the density of delocalized charge carriers in the semiconductor. The method used to accomplish this was to irradiate the semiconductor surface with light from a high intensity microscope lamp. The large photovoltages that developed when the crystals were irradiated indicated that the light was of sufficient energy and intensity to create comparatively large numbers of electron-hole pairs. The effects of unfiltered light upon the open circuit potential-time response of a 2.0 ohm-centimeter crystal in 1.0 N and 0.5 N KOH solutions are shown in Figure 31. Upon irradiation with unfiltered light, the open circuit potential shifted rapidly in the cathodic direction by as much as eight hundred millivolts for the light source used. In order to minimize heating effects, a filter was used to absorb radiation below 360 and above 400 millimicrons. Since an open circuit potential of -650 millivolts was found to be easily attainable, either by varying the voltage to the microscope lamp or by positioning the lamp, this particular open circuit potential was picked as a convenient reference point from which to begin the rate studies in

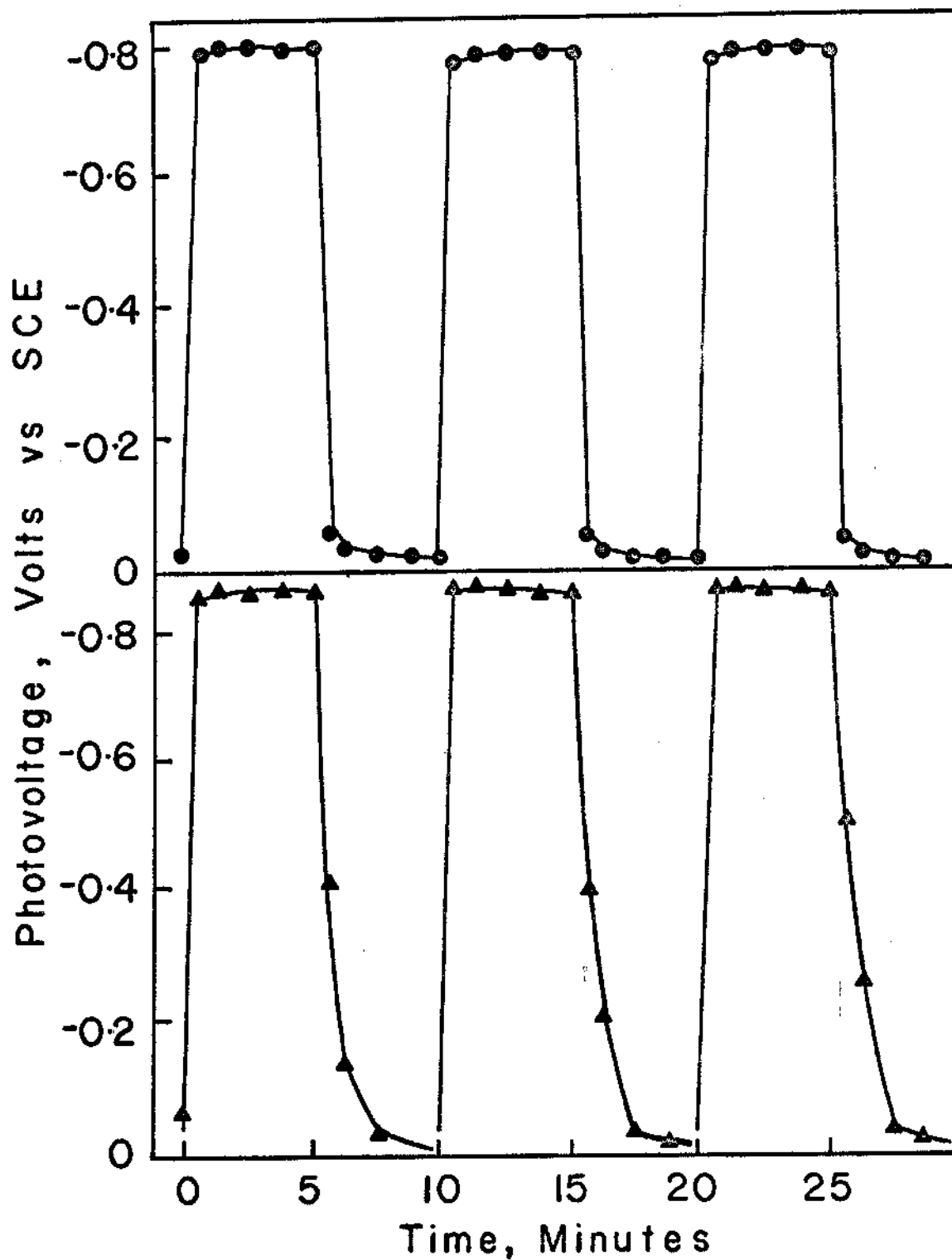


Fig. 31--Change of open circuit potential of a 2.0 ohm-cm ZnO single crystal upon irradiation with light: duration of light pulse was 5 minutes, (●) 0.5 N KOH, (▲) 1.0 N KOH.

the presence of light. After the open circuit potential was maintained at -650 millivolts for about forty-five minutes by adjusting the light intensity, this potential would remain essentially constant for up to forty hours without further adjusting the light source.

The open circuit dissolution rate of the zinc face of the 8.5 ohm-centimeter crystal was then determined in 1.0 N KOH under the presence of light adjusted so as to maintain a constant open circuit potential of -650 millivolts versus SCE. The rate in the presence of light was greater by a factor of almost twice that of the dark dissolution rate. Upon anodic polarization the rate increased by approximately 10 per cent. Upon cathodic polarization the dissolution rates were markedly decreased. The rates were again determined from the slope of plots of milligrams of zinc per  $\text{cm}^2$  (of exposed electrode surface) accumulated in fifty milliliters of 1.0 N KOH versus time, as shown in Figure 32; in the same figure, the rates are also listed as a function of potential. In order to show the close correlation between the dissolution rates as a function of potential and the current-voltage curve (both measured in the presence of light), these two types of data are plotted together in Figure 33. The current density is plotted on the left hand ordinate while the dissolution rates are plotted on the right hand ordinate. It is interesting to note that upon cathodic polarization the dissolution rates in light decrease but do not become smaller than the

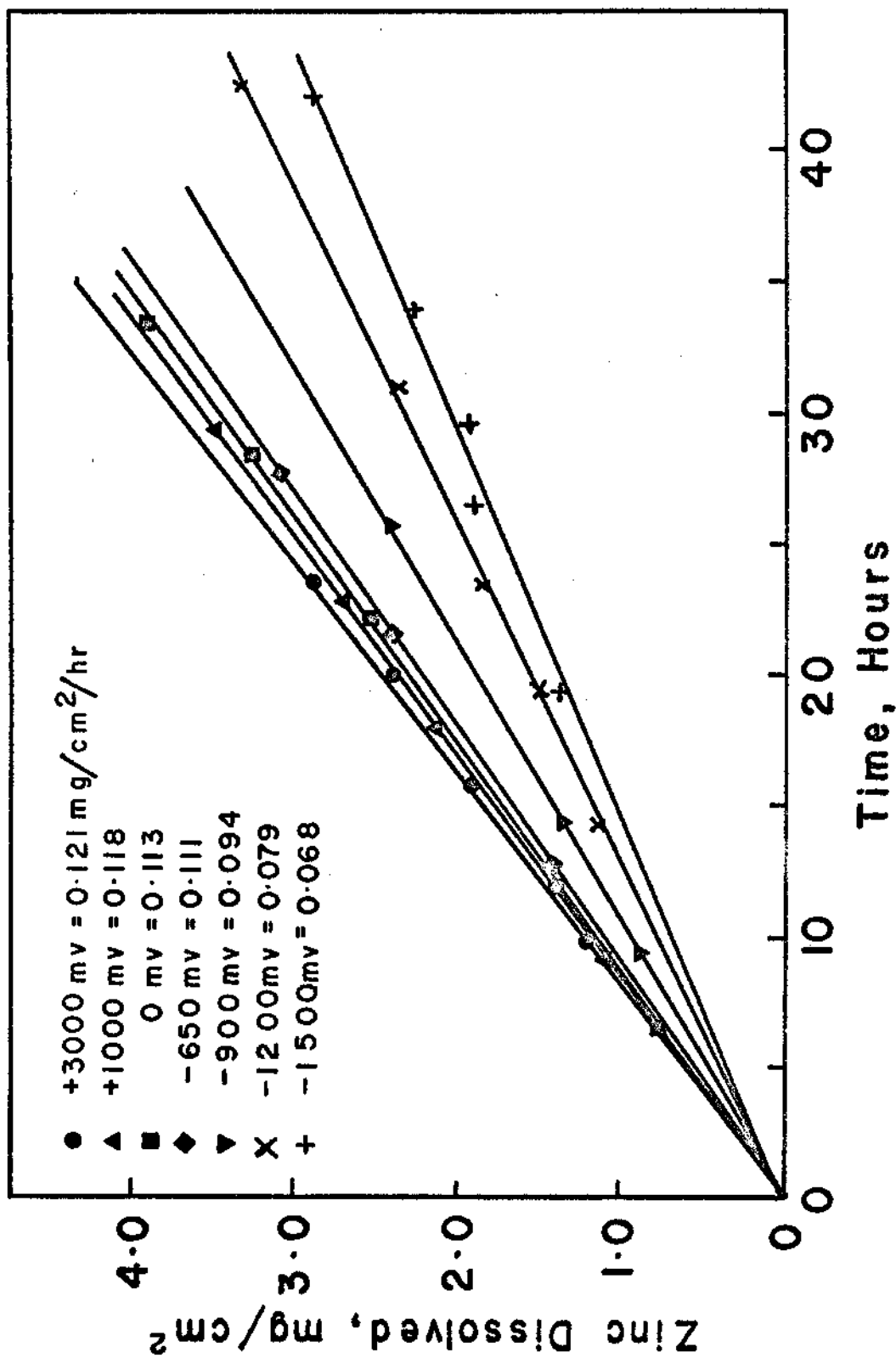
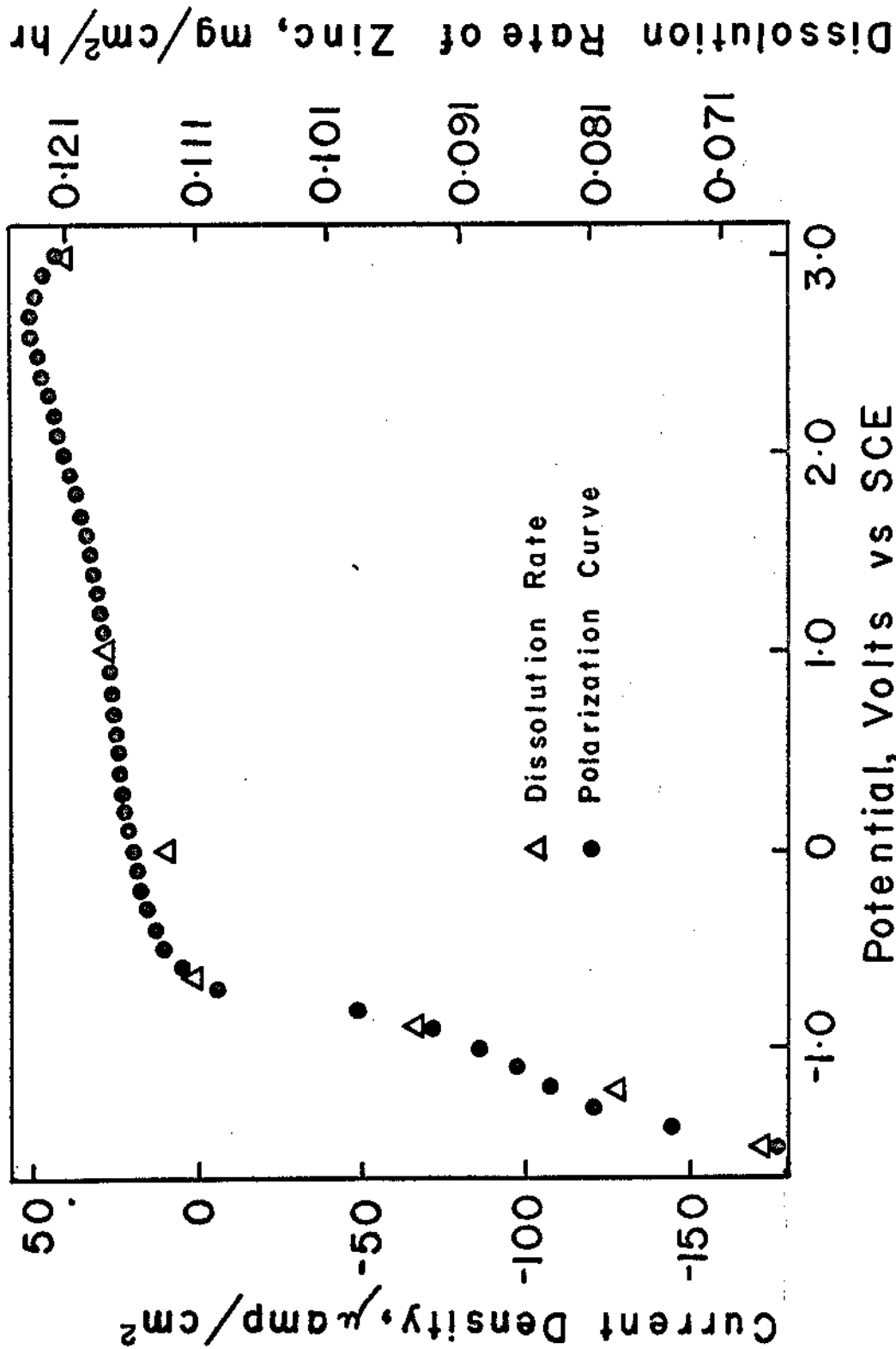


Fig. 32--Dissolution rates as a function of potential for the zinc face of an 8.5 ohm-cm ZnO single crystal in 1.0 N KOH at 31°C. For each rate light was used to adjust the open circuit potential to -650 mv vs SCE.



Potential, Volts vs SCE

Fig. 33--Correlation of zinc dissolution rates with the current-voltage relation for the zinc face of an 8.5 ohm-cm ZnO single crystal in 1.0 N KOH at 31°C. For each rate light was used to obtain an open circuit potential of -650 mv vs SCE.

dissolution rate in the absence of light. Also when the light was turned off, the anodic current dropped by as much as a factor of ten; however, the cathodic current did not change when the light was turned off and on.

In order to measure the effects of electrolyte concentration upon the dissolution rate, the open circuit dissolution rate in light was determined for a 2.0 ohm-centimeter crystal in 0.5 N KOH. This rate was about one-half the corresponding rate in 1.0 N KOH. Upon anodic polarization the dissolution rates again increased; upon cathodic polarization the rates again decreased; however, in 0.5 N KOH the anodic dissolution rates were more markedly increased than in 1.0 N KOH, and the cathodic dissolution rates were less affected than in 1.0 N KOH. These rates in 0.5 N KOH are shown in Figure 34. In order to show the correlation between the dissolution rates as a function of potential and the current-voltage curve, these two types of data are again plotted together as shown in Figure 35. Although there is a correlation between the two types of data, there is not as close a fit for the two types in 0.5 N KOH as in 1.0 N KOH. This may simply be due to the slower dissolution rates in 0.5 N KOH which necessitated either longer periods of time between samples or smaller concentrations of zinc in the samples analyzed. The polarization curves indicated higher anodic currents in 0.5 N KOH than in 1.0 N KOH; the cathodic curves were

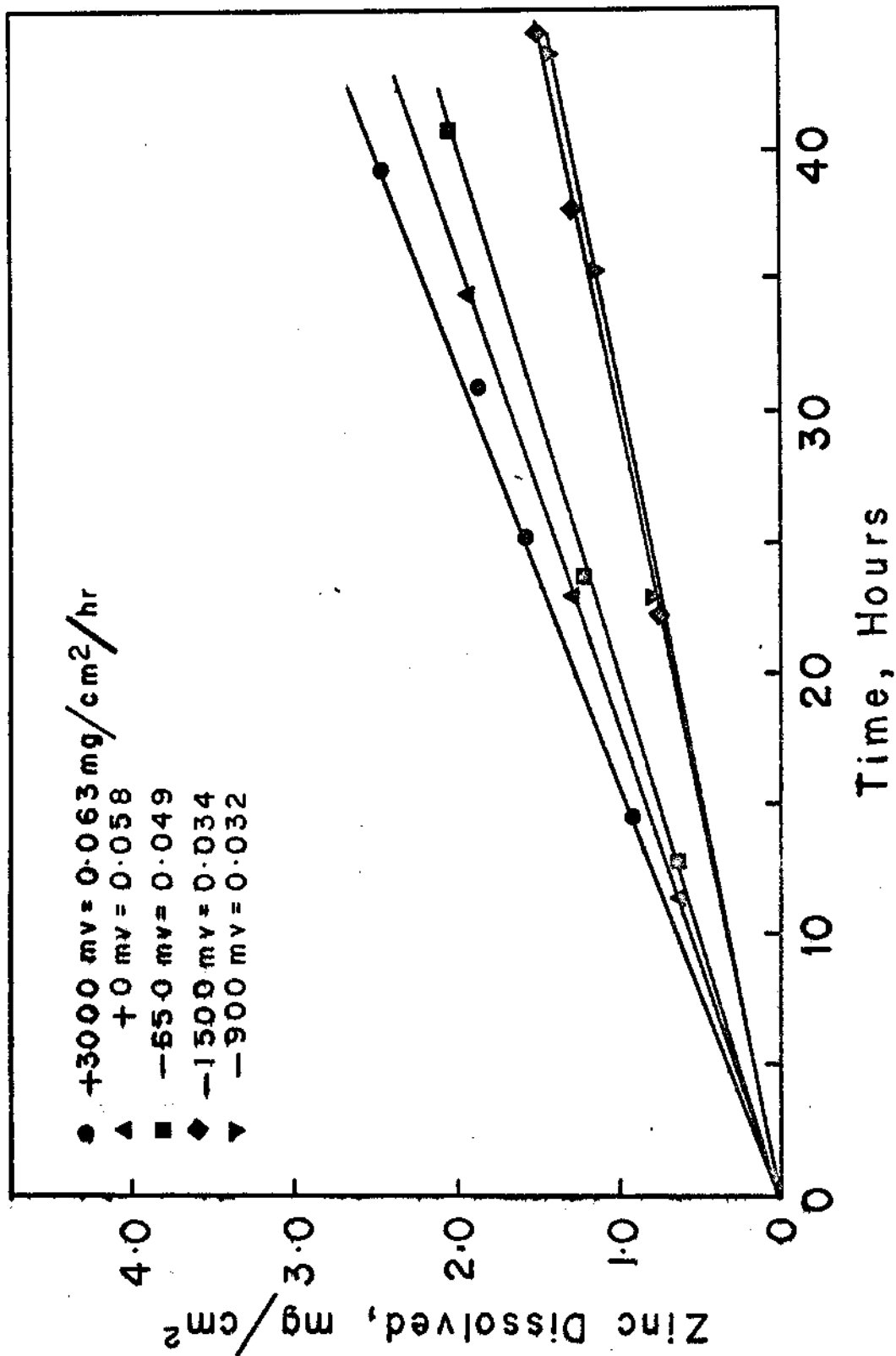


Fig. 34--Dissolution rates as a function of potential for the zinc face of a 2.0 ohm-cm ZnO single crystal in 0.5 N KOH at 31°C. For each rate light was used to adjust the open circuit potential to -650 mv vs SCE.

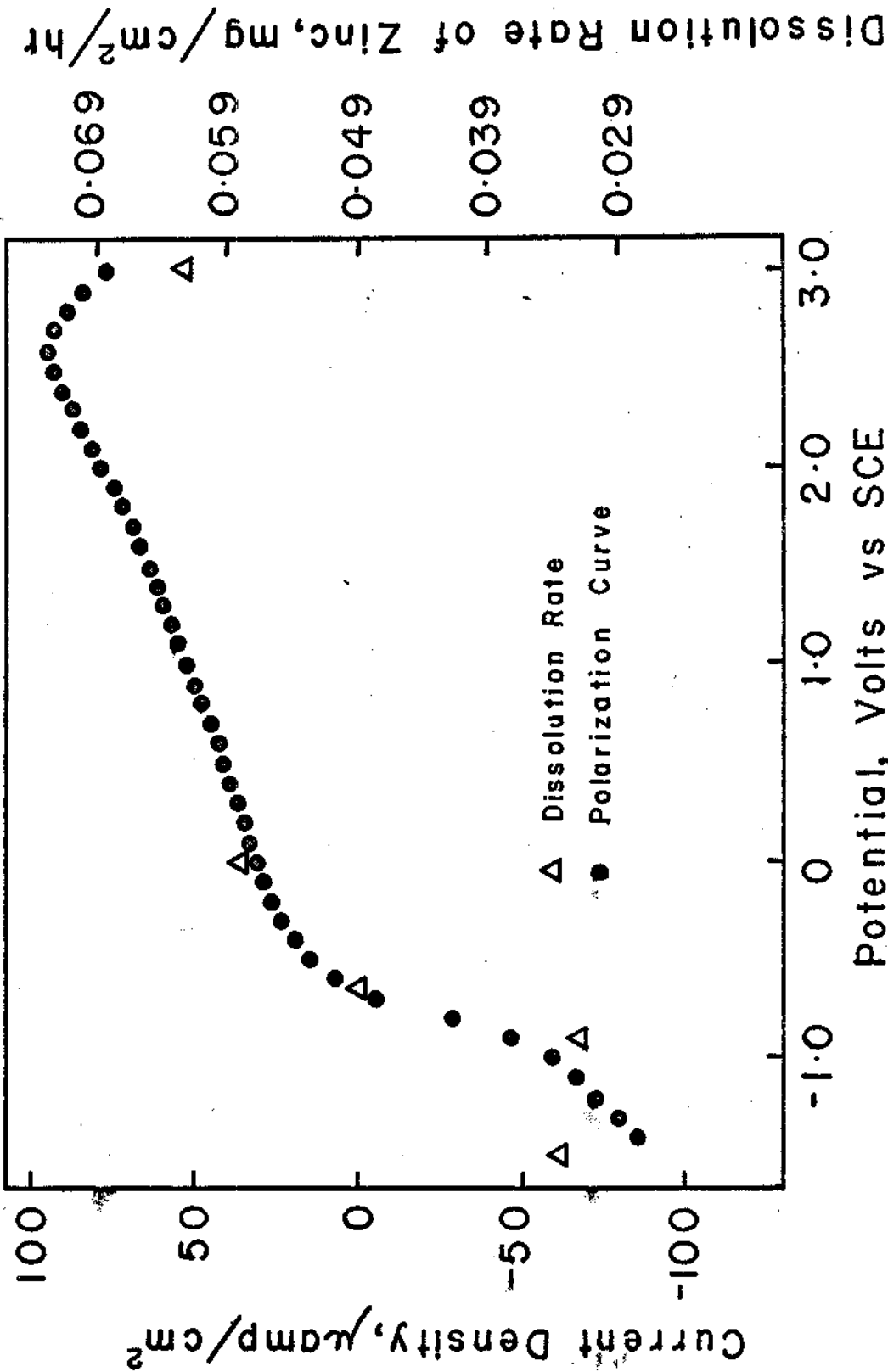


Fig. 35--Correlation of zinc dissolution rates with the current-voltage relation for the zinc face of a 2.0 ohm-cm ZnO single crystal in 0.5 N KOH. For each rate light was used to obtain an open circuit potential of -650 mv vs SCE.



approximately the same for both 0.5 N KOH and 1.0 N KOH. A well defined anodic limiting current was not observed in 0.5 N KOH; at approximately +2700 millivolts, the anodic current decreased slightly with further anodic polarization. The cathodic dissolution rates appeared to reach a limiting value between -900 and -1500 millivolts; both of these potentials were still anodic to the hydrogen evolution region.

In order to determine the influence of resistivity upon the dissolution rates, the open circuit and +3000 millivolt rates were determined for the 2.0 ohm-centimeter crystal under the influence of light. Within experimental error these rates were the same as those found for the 8.5 ohm-centimeter crystal.

The open circuit dissolution rate for the 8.5 ohm-centimeter crystal in 0.5 N KOH was about 30 per cent larger in light than for the corresponding 2.0 ohm-centimeter crystal under the same experimental conditions. Upon anodic polarization the dissolution rates increased even more than for the corresponding points of the 2.0 ohm-centimeter crystal. Again upon cathodic polarization the dissolution rate decreased. Data for calculating the dissolution rates and the rates themselves are shown in Figure 36. Again to show the close correlation between the potential dependent dissolution rates and the current-voltage curve, these two types of data are plotted together in Figure 37. Not only were the dissolution rates

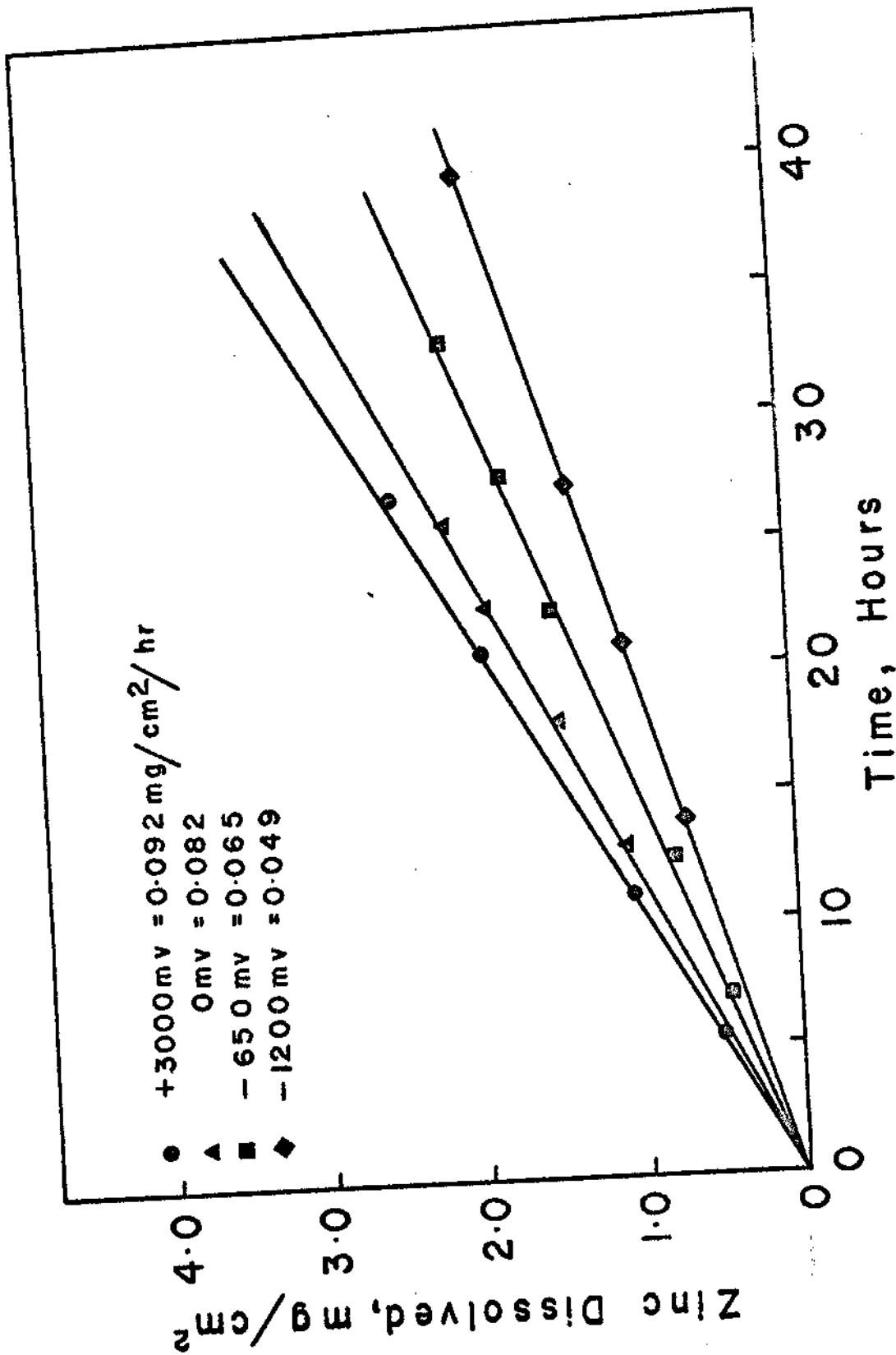


Fig. 36--Dissolution rates as a function of potential for the zinc face of an 8.5 ohm-cm ZnO single crystal in 0.5 N KOH at 31°C. For each rate light was used to adjust the open circuit potential to -650 mv vs SCE.

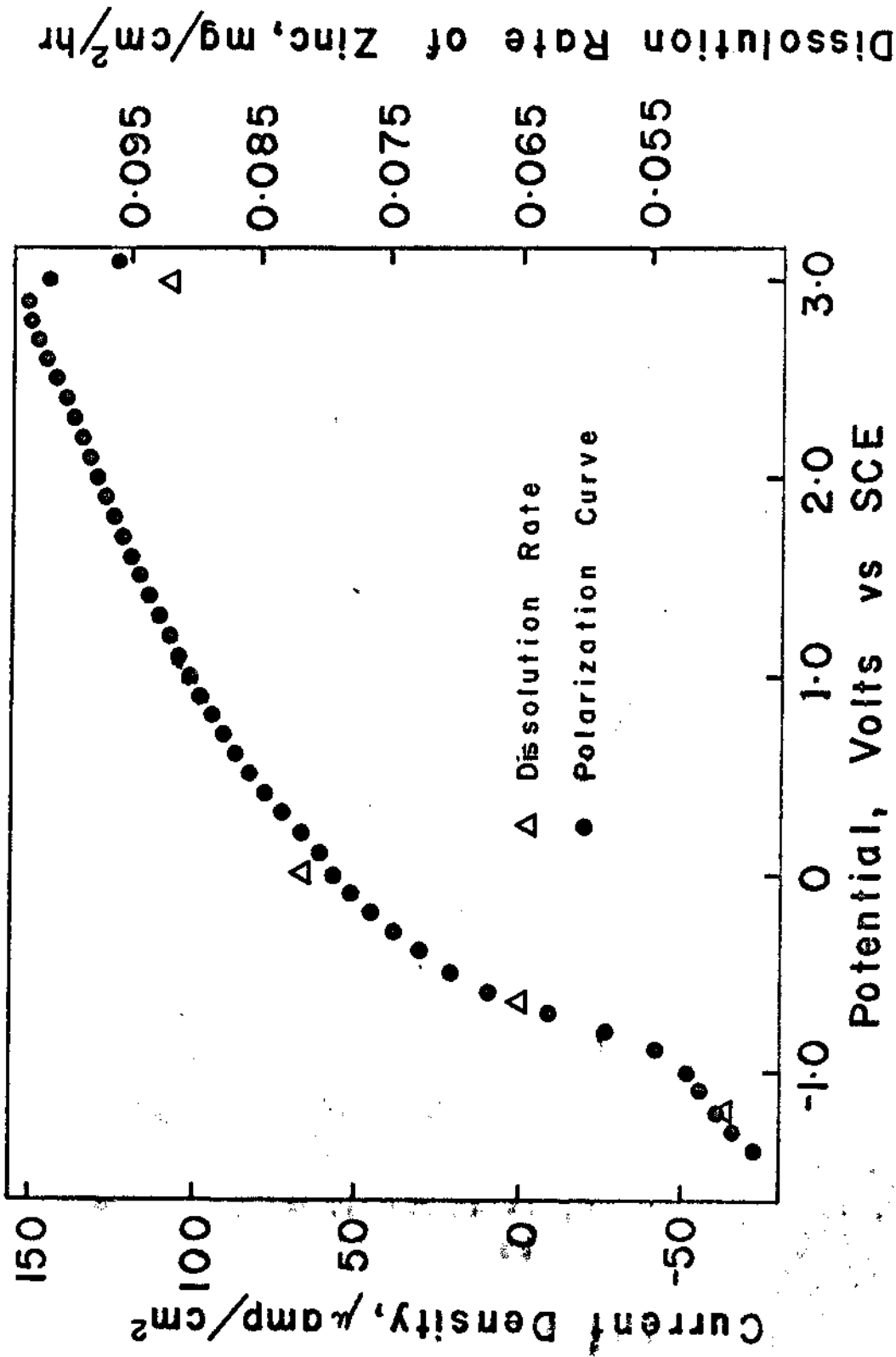


Fig. 37--Correlation of zinc dissolution rates with the current-voltage relation for an 8.5 ohm-cm ZnO single crystal in 0.5 N.KOH at 31°C. For each rate light was used to obtain an open circuit potential of -650 mv vs SCE.

larger for the 8.5 ohm-centimeter crystal in 0.5 N KOH under the influence of light but also the anodic currents of the polarization curve were larger than those for the 2.0 ohm-centimeter crystal. The passive type of peak observed around +2800 millivolts for the 2.0 ohm-centimeter crystal was even more pronounced for the 8.5 ohm-centimeter crystal.

The dissolution rates as functions of potential, concentration, light, and resistivity are summarized in Table II.

Assuming that one or two electrons were given to the conduction band for each zinc atom that went into solution and that these electrons were consequentially measured as an external current flow, the weights of zinc expected in solution after 100 hours of time were calculated; in Table III these values are compared to the actual weights found by analysis. In all cases the amounts determined experimentally were larger than the amounts expected from current measurements.

In order to show more easily the effects of light and electrolyte concentration upon the anodic polarization curves for ZnO, anodic polarization curves obtained under a variety of experimental conditions are shown in Figure 38. The passive type of peak observed at approximately +3000 millivolts in 0.5 N KOH under the influence of light was unexpected; however, from this comparison of polarization data, it can be seen that the peak clearly

TABLE II  
SUMMARY OF DISSOLUTION RATES

Potential mv vs SCE	8.5 ohm-cm in 1 N KOH (light) mg/hr. cm	8.5 ohm-cm in 0.5 N KOH (light) mg/hr. cm	2.0 ohm-cm in 0.5 N KOH (light) mg/hr. cm	8.5 ohm-cm in 1 N KOH (dark) mg/hr. cm
+ 3000	0.121	0.092	0.063	0.068
+ 1000	0.118	.....	.....	.....
0	0.113	0.082	0.058	.....
- 200	.....	.....	.....	0.066
- 650	0.111	0.065	0.049	.....
- 900	0.094	.....	0.032	.....
- 1200	0.080	0.049	.....	0.070
- 1500	0.068	.....	0.034	.....

TABLE III

COMPARISON OF WEIGHT OF ZINC FOUND EXPERIMENTALLY  
TO WEIGHT OF ZINC EXPECTED FROM CURRENT  
MEASUREMENTS

6.5 Ohm-cm in 1.0 N KOH in Light			
Potential Volts vs SCE	( $\int i dt$ )(at, wt. Zn) (1)(F)	( $\int i dt$ )(at, wt. Zn) (2)(F)	Wt. Actually Found
Open Circuit	.....	.....	0.45 mg
0.0	0.22 mg	0.11 mg	0.46
+ 1.0	0.24	0.12	0.49
+ 3.0	0.26	0.13	0.50
8.5 Ohm-cm in 1.0 N KOH in Darkness			
Open Circuit	.....	.....	0.26 mg
+ 3.0	0.01 mg	0.005 mg	0.26
8.5 Ohm-cm in 0.5 N KOH in Light			
Open Circuit	.....	.....	0.25 mg
0.0	0.17 mg	0.09 mg	0.32
+ 3.0	0.28	0.14	0.36
- 1.2	.....	.....	0.19
2.0 Ohm-cm in 0.5 N KOH in Light			
Open Circuit	.....	.....	0.19 mg
0.0	0.10 mg	0.05 mg	0.23
+ 3.0	0.20	0.10	0.25
- 1.2	.....	.....	0.12

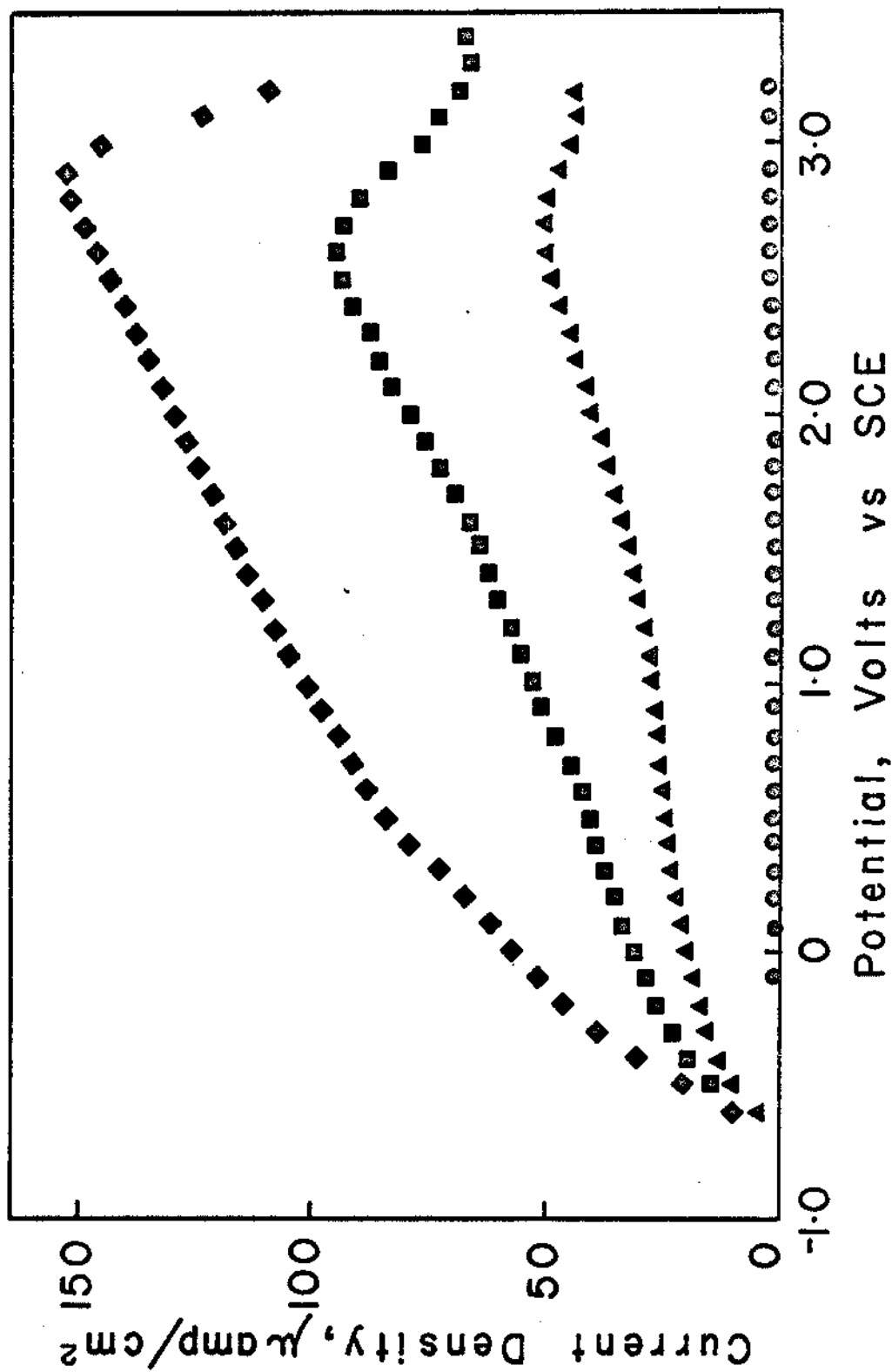


Fig. 38--Comparison of anodic current-voltage curves for the zinc face of ZnO single crystal electrodes; (●) 8.5 ohm-cm crystal in the dark in 1.0 N KOH, (▲) 8.5 ohm-cm crystal in light in 1.0 N KOH, (◆) 2.0 ohm-cm crystal in light in 0.5 N KOH, (■) 8.5 ohm-cm crystal in light in 0.5 N KOH.

became more pronounced as the current density of the polarization curve increased.

When the potential was moved from open circuit potentials to more anodic values and then moved from these anodic values back to open circuit, the same shape anodic polarization curves and the same current magnitudes were obtained. When the potential was moved from open circuit to cathodic values more negative than -1500 millivolts versus SCE, curves such as the bottom curve of Figure 39 were obtained. When the potential was moved from these highly cathodic values back toward open circuit, the hydrogen evolution curve went into an anodic pseudo-passive peak as shown by the top curve of Figure 39. This peak was present whether or not zinc ions were present in solution. The height of this peak decreased with time until a cathodic current was again measured.

Anodic polarization curves did not fit a Tafel plot. When the cathodic potential was plotted versus the logarithm of the corresponding current, a somewhat straight line was obtained between approximately -800 millivolts and -1500 millivolts versus SCE; however, the slope had no meaning in connection with the Tafel relation. In the region between about -1650 and -1900 millivolts, the current increased very rapidly; at approximately -1700 millivolts, hydrogen gas evolution was clearly visible. Starting about -1500 millivolts, the cathodic currents



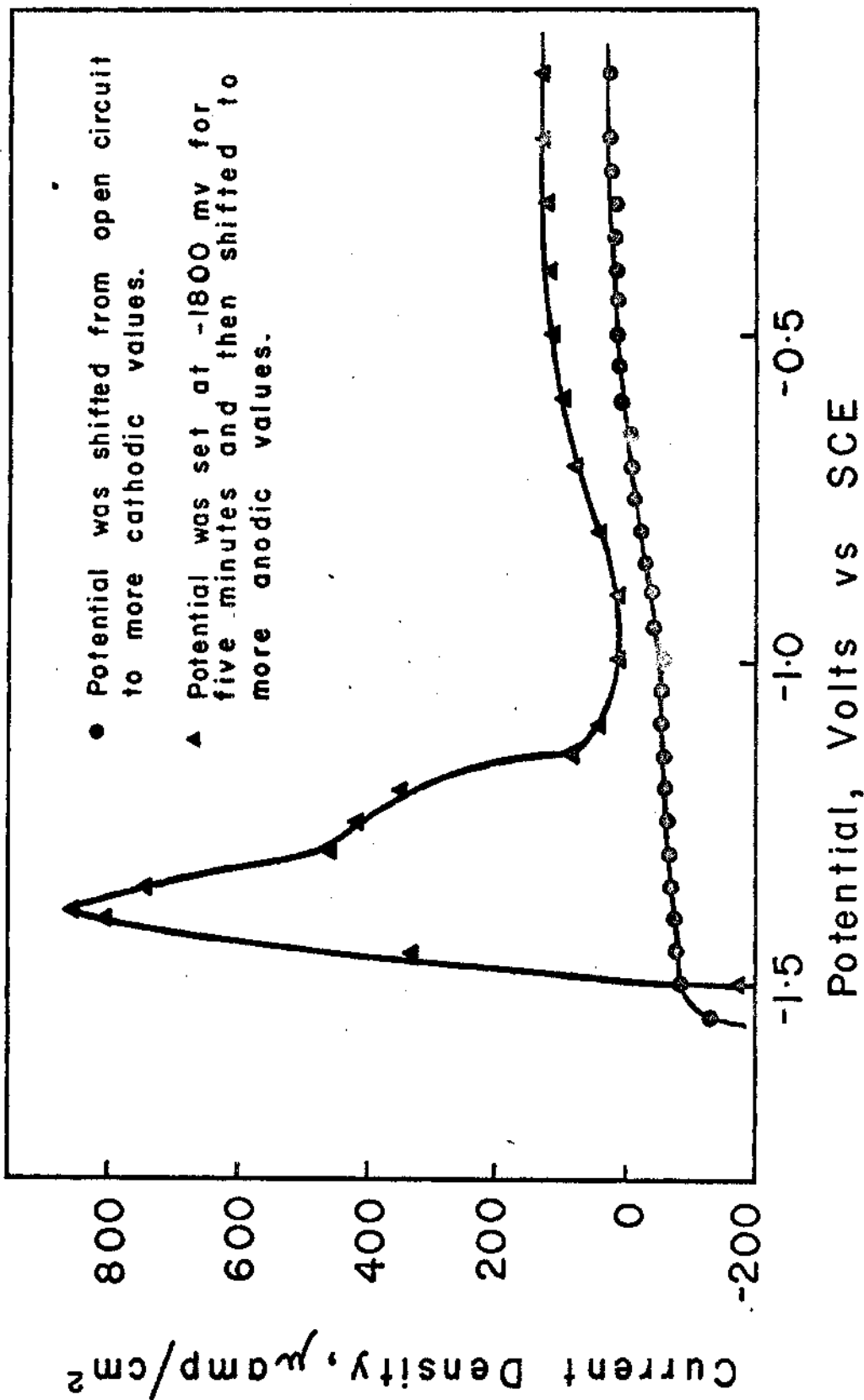


Fig. 39--Potentiostatic current-voltage curves of a 2.0 ohm-cm ZnO single crystal in 1.0 N KOH at 31°C.

became large enough for resistance polarization to become important. Plots of cathodic potential versus logarithm of the current are shown in Figure 40. The curves were corrected for IR potential drops in the semiconductor. Although the cathodic currents did not increase over the three orders of magnitude which are necessary to accurately establish a Tafel plot, the slope of the potential-logarithm of the current curve was measured and found to be approximately  $100 \pm 20$  millivolts per decade of current. The shapes of all the cathodic polarization curves were in general the same regardless of experimental conditions; even the magnitudes of the cathodic currents were approximately the same.

In order to determine if large potential drops occurred in the Helmholtz layer upon changes in pH, the open circuit potential was measured as a function of pH. When the electrode was maintained in the absence of light, the potential did not change much as shown by the lower curve of Figure 41. For the upper curve light was used to obtain an open circuit potential of about -800 millivolts in 1 N KOH; sulfuric acid was then titrated into the solution. In the pH range between eight and fourteen, the potential changed at the rate of about 74 mv per pH as the solution was made more acidic. As the solution was made even more acidic, the open circuit potential leveled off at about -300 millivolts between

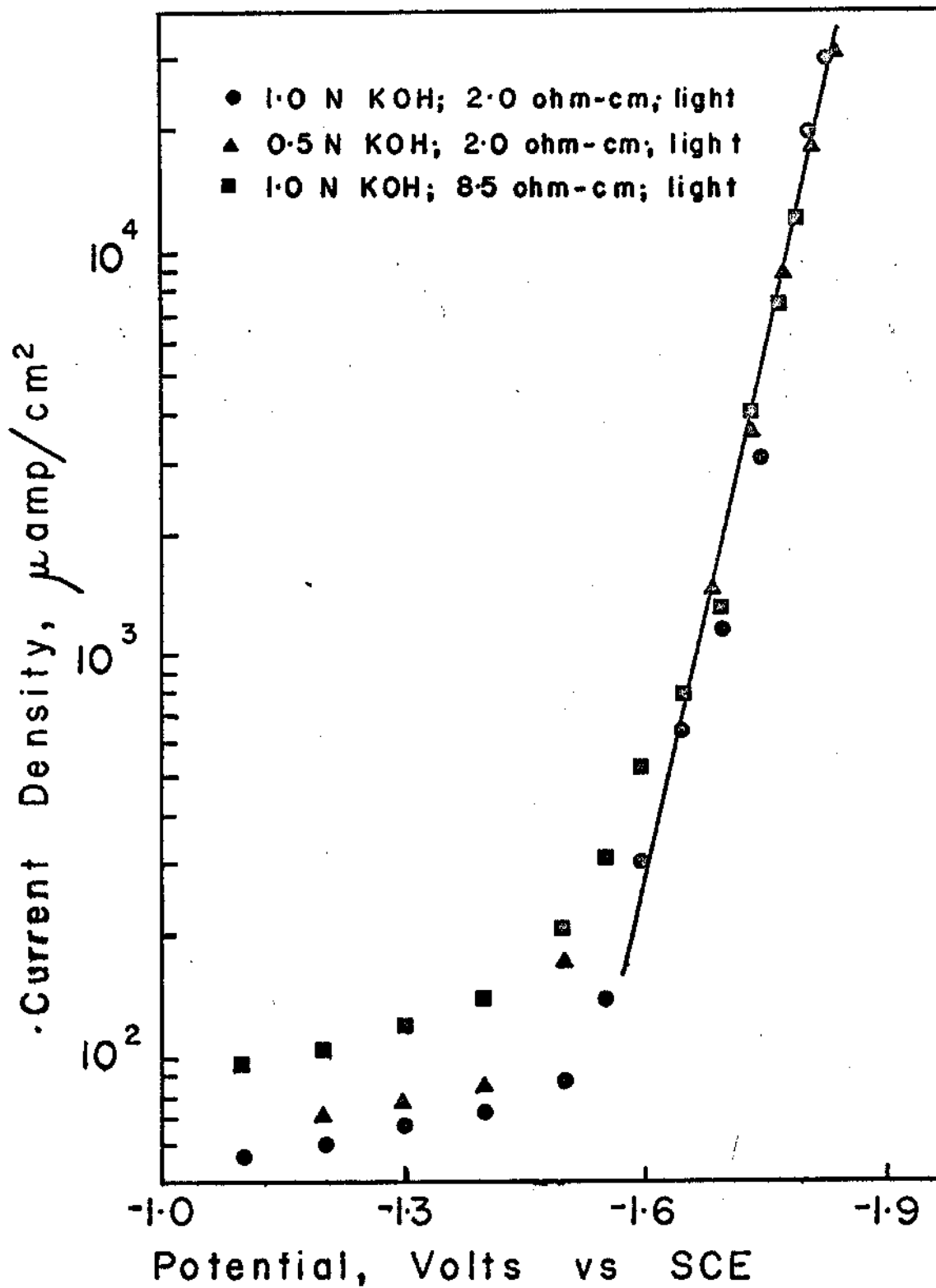


Fig. 40--Comparison of cathodic current-voltage curves of ZnO electrodes.

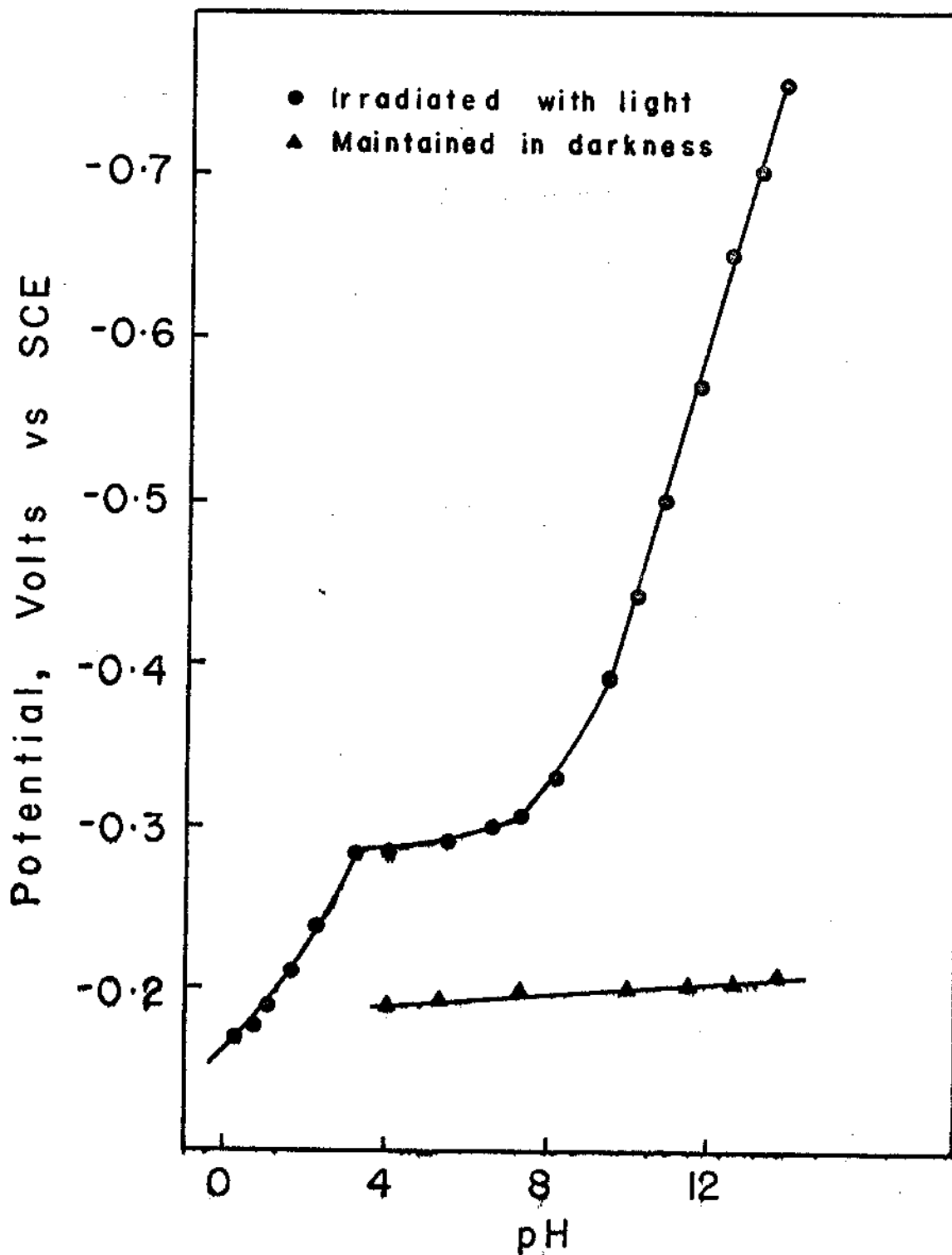


Fig. 41--Effect of light upon potential-pH curves of the zinc face of an 8.5 ohm-cm ZnO single crystal electrode.

pH values of eight to three. At values more acidic than pH 3, the open circuit potential shifted slowly toward more anodic values. In sulfuric acid solutions the crystal was observed to quickly dissolve with the most rapid dissolution occurring along the edges; etch pits were not observed in the flat surface.

Etching pits observed on the zinc face in 0.5 N and 1.0 N KOH were very small and appeared to progress in lines parallel to the edges of the crystals. No definite difference could be seen in the pitting as a function of potential. A typical photomicrograph of a zinc face after exposure to an alkaline solution is shown in Figure 42.

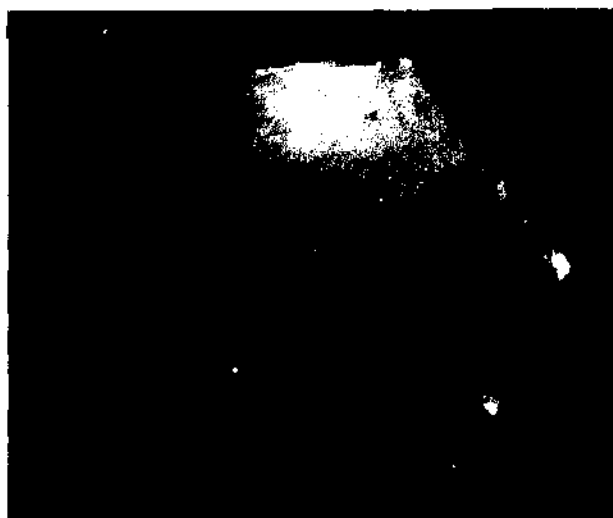


Fig. 42--Photomicrograph of zinc face of single crystal ZnO after exposure to 1.0 N KOH for 40 hours in light, open circuit conditions, 45X magnification.

## CHAPTER VI

### CONCLUSION

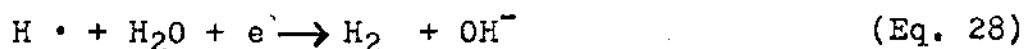
The results of the present study can be related through at least five properties to the electrochemical dissolution of other semiconductors and metals. Although the five properties are interrelated, they can, for clarification, be divided into the topics of passivity phenomenon, hydrogen gas evolution, capacity measurements, photovoltaic activity, and finally dissolution rates.

#### Passivity Phenomenon

The passive peak observed at approximately +3000 mv in the polarization curves may have been the result of zinc ion concentrations which exceeded the solubility product of  $Zn(OH)_2$  in the Helmholtz layer and which produced a precipitated film on the ZnO surface. It is interesting that when anodic polarization curves were compared, the passive peak became more pronounced with increasing current densities in the polarization curves. As in some metals and as in silicon a film was decreasing the probability of charge transfer across the solid-solution interface; however, additional work is needed to establish the nature of this film.

### Hydrogen Gas Evolution

At approximately -1700 mv hydrogen gas evolution was clearly visible. At these cathodic potentials adsorbed water molecules with the hydrogen portion of the molecules directed toward the ZnO surface will almost completely cover the surface. Electron transfer occurs from the conduction band of ZnO to these adsorbed water molecules. Although the Tafel plot does not clearly indicate the number of electrons exchanged, the following reactions probably occur:



The hydrogen atoms thus produced may diffuse to some extent into the crystal, or zinc may be reduced to metallic zinc at the surface. In any case as the potential was made more anodic, electrons were easily lost to the conduction band and measured as an anodic current which diminished with time until cathodic currents were again measured. These data agree with the different capacity curves measured for the two directions of polarization by Blok (1, p. 96).

### Capacity Measurements

Changes in measured open circuit potentials reflect changes in the space charge layer of semiconductors; thus, changes in open circuit potential as functions of time and

light irradiation can be interpreted in terms of existing capacity measurements. The slow shift in open circuit potential of freshly polished crystals toward more anodic values was due to the slow adsorption of hydroxide ions onto the exposed ZnO surface. This adsorption altered the charge distribution at the semiconductor-solution interface from flat-band conditions which prevailed immediately upon immersion to higher densities of positive charges in a space charge region. This can be pictured as an upward bending of the energy bands, as discussed in Chapter II. The measured open circuit potential slowly changed as a result of these alterations in charge distribution. After the crystal was kept in KOH for a period of time and then exposed to room air, a film of adsorbed oxygen developed. Adsorbed oxygen atoms cause even more upward bending than hydroxide ions (7, p. 283); the small shift from about -150 to -200 mv upon immersion of the crystal may have been the result of the displacement in KOH of this film by hydroxide ions. Similar results have been reported for silicon (5).

From capacity measurements the flat-band potential of ZnO in 1.0 N KOH is approximately -700 mv vs SCE (6). The open circuit potential of -650 mv obtained by irradiating the surface with light was thus about 50 mv or so anodic to flat-band potential; thus, an anodic space charge layer existed to some extent inside the crystal even at open circuit. Also, the flat-band potential



changes to more anodic potentials at the rate of 54 mv per pH unit (6); therefore, in 0.5 N KOH the open circuit potential of -650 mv was closer to the flat-band potential than it was in 1.0 N KOH, and at open circuit a smaller space charge layer existed in the crystal. The flat-band potential also moves toward more anodic potentials at the rate of about 50 mv per power of ten decrease in electron density (2). Since conductivity decreases with a decrease in electron density and resistivity is the reciprocal of conductivity, crystals with larger resistivity values have more anodic flat-band potentials. Thus at the open circuit potential of -650 mv, an even smaller anodic space charge layer existed in the 8.5 ohm-cm crystal than in the 2.0 ohm-cm crystal. In the interpretation of the potential dependent ZnO dissolution rates in light, the importance of this space charge and the influence of applied potentials upon the width of this region will be discussed in more detail.

Before discussing dissolution rates, the importance of the space charge region can be seen by examining the pH-potential curves in both darkness and in light. In both the presence and absence of light, the capacity of the space charge layer is essentially determined by donor atoms; as the pH decreases, the capacity minimum shifts toward more anodic values (6). In the absence of light the measured pH-potential curve did not appreciably change because very few electron-hole pairs were produced in the

dark, and thus their distribution did not change greatly as the pH changed. A strong space charge layer already existed, and only the depth of ionized donor ions changed. When ZnO was irradiated, the capacity of the space charge was still essentially controlled by donor atoms and did not change very much from that found in the dark (4, 8). However, the number of electron-hole pairs was greatly increased by light; at an open circuit potential of -750 mv in 1.0 N KOH, the ZnO crystal was close to flat-band conditions. Since the distribution of electron-hole pairs is controlled by the electrical field in the donor space charge, which changes as the pH changes, there was a more marked change of surface hole density in light and thus of measured open circuit potential.

#### Photovoltage

The fact that large cathodic photovoltages were observed upon irradiation of ZnO with light indicates that the open circuit potential was under mixed control and that the anodic half-cell reaction was greatly increased by light in agreement with the photovoltaic effect discussed in Chapter II. This indicates that an electrochemical process was occurring but that in the dark it was much smaller than an accompanying chemical process.

#### Dissolution Rates

Measured dark dissolution rates between the potentials of -1500 mv and +3000 mv were independent of potential and

thus predominately chemical in nature. The large photovoltages measured upon irradiation of the crystals with light indicates that comparatively large numbers of electron-hole pairs were produced; the increase of dissolution upon irradiation shows that one of these delocalized charge carriers (holes) was involved in the dissolution process.

The following situation can be envisioned to interpret the influence of holes upon the dissolution rates. When a crystal is adjusted by light so that the open circuit potential corresponds to the flat-band potential, the electron-hole pairs produced by light diffuse about in the crystal; part of them diffuse to the surface and take part in the two half-cell reactions occurring there, and part of them recombine. When the crystal is made anodic to the flat-band potential (either by the electrolyte or by applied potentials), a strong electrical field is built up in the space charge layer. This field separates electrons and holes generated in the region (3). When an anodic potential is applied to the crystal, electrons from the separated electron-hole pairs are forced toward the semiconductor-metal contact and then through the external circuit where a net current is measured while the separated holes are forced to the surface and take part in the dissolution process. Some electron-hole pairs from beyond the space charge layer may diffuse into the region; however, beyond the space charge region the recombination

probability is high because of the very low field strength. The electrochemical portion of the dissolution rate is determined by the number of electron-hole pairs produced and separated in the space charge region.

Support for this concept can be obtained by examining the dissolution rates in relation to the flat-band potential obtained by capacity measurements. As mentioned previously the open circuit potential of -650 mv for the 8.5 ohm-cm crystal in 1.0 N KOH was about 50 mv or so anodic to the flat-band potential. A space charge existed in the crystal, and the portion of holes produced in this region was forced to the surface even at open circuit. Upon anodic polarization the surface hole density was additionally increased by increasing the depth from which holes were forced to the surface; the anodic current and dissolution rates parallel this increase in surface hole density. Upon cathodic polarization the energy bands can be pictured as being changed from upward bending at open circuit, through the flat-band potential, and then being forced to downward bending. This reflects a large decrease in surface hole density which parallels a sharp decrease in the measured cathodic dissolution rates.

For the 2.0 ohm-cm crystal in 0.5 N KOH, the open circuit potential of -650 mv was still anodic to flat-band potential but not as much so as in 1.0 N KOH. At open circuit a smaller space charge layer existed in the crystal, and a smaller portion of light produced holes

were thus being forced to the surface compared to open circuit in 1.0 N KOH solutions. More holes were available to be forced to the surface by anodic polarization; fewer holes were available to be forced back from the surface by cathodic polarization. The lower total dissolution rate was the result of a decrease in the chemical dissolution rate with a decrease in hydroxide ion concentration.

For the 8.5 ohm-cm crystal in 0.5 N KOH, the open circuit potential of -650 mv was even closer to the flat-band potential than either the 2.0 ohm-cm crystal in 0.5 N KOH or the 8.5 ohm-cm crystal in 1.0 N KOH; an even smaller anodic space charge region existed at open circuit, and a smaller portion of holes moved to the surface. Upon anodic polarization a larger portion was available to be forced to the surface, and upon cathodic polarization a smaller portion was available to be forced back from the surface. The measured dissolution rates parallel this concept, as do also the experimentally determined polarization curves.

Additional evidence for the importance of the space charge region can be seen from a plot of  $i^2$  versus  $\eta$ . As shown in Figure 43, such a plot gives reasonably straight lines from open circuit to approximately +200 mv. From semiconductor theory the width of the space charge region increases with  $\sqrt{\eta}$ . The polarization curves can then be interpreted from the point of view that the

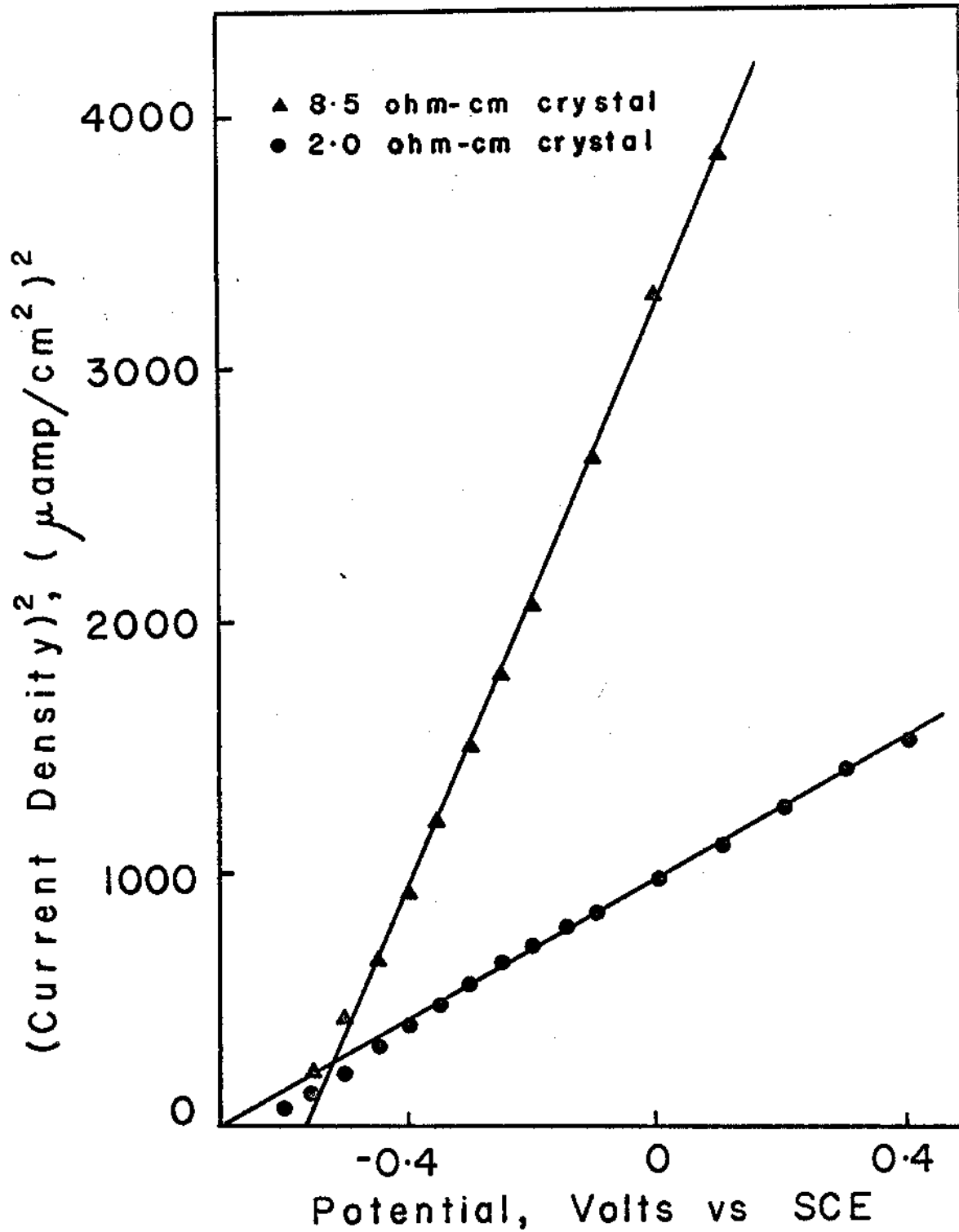
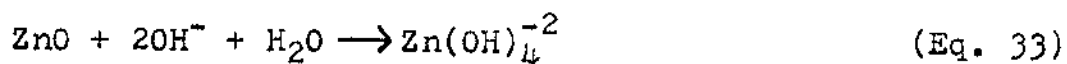
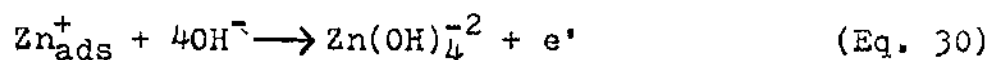


Fig. 43--Effect of resistivity upon the linear relation between the square of current vs potential for the zinc face of ZnO single crystals in light in 0.5 N KOH.

photocurrent increases with  $\sqrt{\eta}$ , that is, with the increase in width of the space charge region. An equivalent relationship between capacity and photocurrent has been reported for CdS (9).

#### Proposed Dissolution Mechanism

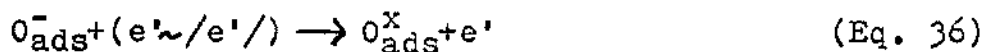
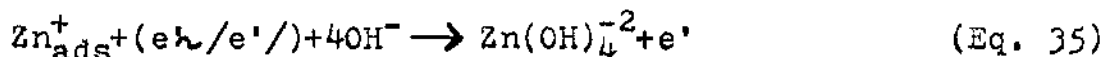
The dark dissolution processes between -1.5 volts and +3 volts have been shown to be independent of potential and thus chemical in nature. The chemical processes can be described by the following reactions:



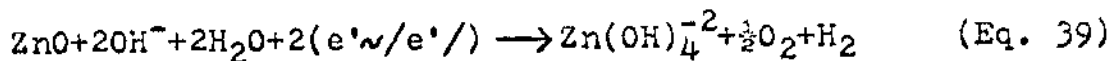
In the proposed chemical dissolution process, there is a transfer of an electron from zinc to oxygen as the result of a strong localized electrical field established by adsorbed hydroxide ions on the zinc surface. The step is a direct transfer because most of the electrons do not have enough energy to be delocalized to the higher lying conduction band; however, a very small portion does have enough energy to make the transition. This can be considered to be electron-hole pair production which

causes the mixed potential measured at open circuit even in the dark. Applied potentials can not add enough energy to measurably increase the portion of electrons that has enough energy to make the transition. In addition, applied voltages influence mainly the space charge region of the semiconductor and appear only to a limited extent across the semiconductor-solution interface. The composition of the phase at the semiconductor-solution interface does not change, and thus the localized electrical field established by adsorbed ions is not changed.

The fact that the weight of zinc actually measured in solution was always greater than the amount expected from current measurements shows that a potential independent dissolution process (chemical dissolution) continues even in light; however, an additional dissolution process involving holes increases the total dissolution process. A mechanism such as the following can be envisioned for this potential dependent (electrochemical dissolution) process.

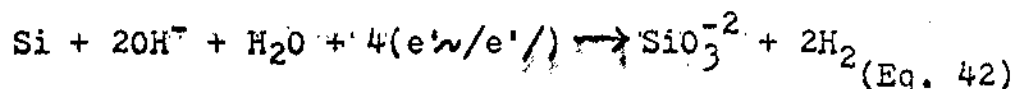
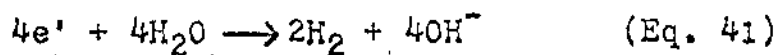
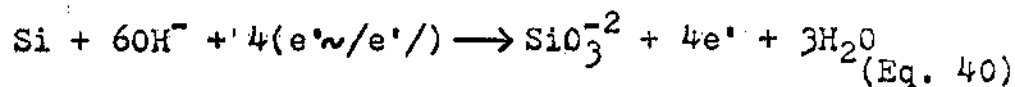






where  $(e' \backslash / e' /)$  represents an electron-hole pair. In these reactions electrons are delocalized to the conduction band; the potential dependent step is the arrival of holes at the semiconductor surface.

The proposed electrochemical dissolution process actually is analogous to the electrochemical dissolution of germanium and silicon except that in the proposed reactions for ZnO light energy decomposes a mole of water into its constituent elements for each mole of ZnO that dissolves electrochemically. This can be seen more clearly if the half-cell reactions for silicon dissolution are written in a slightly different fashion from that used in the original papers. The following reactions for silicon can be compared with the proposed electrochemical dissolution of ZnO:



Electron-hole pairs are necessary for the electrochemical dissolution. In germanium and silicon the forbidden gap is small enough so that applied potentials can generate

electron-hole pairs whereas in ZnO the forbidden gap is so large that applied potentials of the magnitude used in this study can not generate electron-hole pairs but can only alter the distribution of those produced by light.

Additional chemical data are needed to establish these proposed chemical and electrochemical mechanisms; in particular, very precise measurements of the rates of evolution of hydrogen and oxygen gases are needed. In order to further clarify the dissolution processes, dissolution rates could be determined in the dark for crystals with lower resistivities in an attempt to localize applied potentials across the semiconductor-solution interface. When a potential is applied to a semiconductor, most of the potential drop occurs in the space charge layer of the semiconductor; however, at high overpotentials, large potential drops can occur in the Helmholtz layer and can become comparable in magnitude to those in the space charge layer. Dissolution rates could be measured at very strong anodic potentials in an attempt to determine if the composition of the Helmholtz layer can be altered enough to change the dissolution rate. The type of work presented in the present paper could also be extended to a series of semiconductors selected on the basis of the width of the forbidden gap of the compound in an effort to determine where and if the dark dissolution processes in the series are potential dependent.

## CHAPTER BIBLIOGRAPHY

1. Blok, L., The Ionic Double Layer on Zinc Oxide in Aqueous Electrolyte Solutions, "Bronder-Offset" Rotterdam, 1968.
2. Dewald, J. F., "Charge and Potential Distribution at the Zinc Oxide Electrode," The Bell System Technical Journal, XXXIX (May, 1960), 615-639.
3. Gerischer, H., "Electrochemical Behavior of Semiconductors under Illumination," Journal of the Electrochemical Society, CXIII (November, 1966), 1174-1180.
4. Hauffe, Von K. and Range, J., "Über die anodische Auflösung von Zinkoxid-Einkristallen unter Lichteinwirkung," Berichte der Bunsengesellschaft, LXXI (July, 1967), 690-697.
5. Izidinou, S. U. and others, "Electrochemical and Photoelectrochemical Behavior of the Silicon Electrode," Doklady Akademii Nauk S.S.S.R., CXXXIII (July, 1960), 392-395.
6. Lohmann, F., "Der Einfluss des pH auf die Elektrischen und Chemischen Eigenschaften von Zinkoxidelektroden," Berichte der Bunsengesellschaft, LXX (April, 1966), 428-434.
7. Morrison, S. R., Surface Barrier Effects in Adsorption, Illustrated by Zinc Oxide, Vol. VII of Advances in Catalysis, edited by W. G. Frankenburg, E. K. Rideal and V. I. Komarewsky (13 volumes), New York, Academic Press, Inc., 1955.
8. Morrison, S. R. and Freund, T., "Chemical Role of Holes and Electrons in ZnO Photocatalysis," The Journal of Chemical Physics, VLII (August, 1967), 1543-1551.
9. Tyagai, V. A., "Study of the Nature of a Pulsed Photoeffect at a Cadmium Sulfide-Electrolyte Solution Interface," Soviet Physics-Solid State, VI (December, 1964), 1260-1264.

## BIBLIOGRAPHY

### Books

- Blok, L., The Ionic Double Layer on Zinc Oxide in Aqueous Electrolyte Solutions, "Bronder-Offset" Rotterdam, 1968.
- Brown, H. E., Zinc Oxide Rediscovered, New York, The New Jersey Zinc Company, 1957.
- Hannay, N. B., Semiconductors, New York, Reinhold Publishing Corporation, 1959.
- Henisch, H. K., Rectifying Semiconductor Contacts, Oxford, Oxford University Press, 1957.
- Morrison, S. R., Surface Barrier Effects in Adsorption, Illustrated by Zinc Oxide, Vol. VII of Advances in Catalysis, edited by W. G. Frankenburg, E. K. Rideal and V. I. Komarewsky (13 volumes), New York, Academic Press, Inc., 1955.
- Myamlin, V. A. and Pleskou, Y. V., Electrochemistry of Semiconductors, New York, Plenum Press, 1967.
- Vetter, K. J., Electrochemical Kinetics, Theoretical and Experimental Aspects, New York, Academic Press, 1967.

### Articles

- Beck, F. and Gerischer, H., "Zum Mechanismus der Anodischen Auflosung von Germanium in Alkalischer Losung," Zeitschrift fur Elektrochemie, LXIII (April, 1959), 500-510.
- Brattain, W. and Garrett, C., "The Interface Between Germanium and an Electrolyte," The Bell System Technical Journal, XXXIV (January, 1955), 129-177.
- Dewald, J. F., "Charge and Potential Distribution at the Zinc Oxide Electrode," The Bell System Technical Journal, XXXIX (May, 1960), 615-639.

- Florianovich, G. M. and Kolotyrkin, Y. M., "On the Problem of the Mechanism of the Solution of Iron Alloys with Chromium in Sulfuric Acid," Doklady Akademii Nauk SSSR, CLVII (July, 1964), 422-425.
- Gerischer, H., "Electrochemical Behavior of Semiconductors under Illumination," Journal of the Electrochemical Society, CXIII (November, 1966), 1174-1180.
- Hauffe, Von K. and Range, J., "Über die anodische Auflösung von Zinkoxid-Einkristallen unter Lichteinwirkung," Berichte der Bunsengesellschaft, LXXI (July, 1967), 690-697.
- Hurd, R. M. and Wrotenbery, P. T., "Electrochemistry of the Silicon-Electrolyte Interface," Annals of the New York Academy of Science, CI (January, 1963), 876-903.
- Izidinou, S. U. and others, "Electrochemical and Photoelectrochemical Behavior of the Silicon Electrode," Doklady Akademii Nauk SSSR, CXXXIII (July, 1960), 392-395.
- Lohmann, F., "Der Einfluss des pH auf die Elektrischen und Chemischen Eigenschaften von Zinkoxidelektroden," Berichte der Bunsengesellschaft, LXX (April, 1966), 428-434.
- Mariano, A. N. and Hanneman, R. E., "Crystallographic Polarity of ZnO Crystals," Journal of Applied Physics, XXXIV (February, 1963), 384-388.
- Mohanty, G. P. and Azaroff, L. V., "Electron Density Distributions in ZnO Crystals," The Journal of Chemical Physics, XXXV (October, 1961), 1268-1270.
- Morrison, S. R. and Freund, T., "Chemical Role of Holes and Electrons in ZnO Photocatalysis," The Journal of Chemical Physics, VLII (August, 1967), 1543-1551.
- Oakes, G. and West, J. M., "Influence of Thiourea on the Dissolution of Mild Steel in Strong Hydrochloric Acid," British Corrosion Journal, IV (March, 1969), 66-73.
- Parks, G. A. and de Bruyn, P. L., "The Zero Point of Charge of Oxides," Journal of Physical Chemistry, LXVI (October, 1962), 967-973.
- Scharowsky, E., "Optische und elektrische Eigenschaften von ZnO-Einkristallen mit Zn-Überschuss," Zeitschrift für Physik, CXXXV (June, 1953), 318-330.

- Szigeti, B., "Polarizability and Dielectric Constant of Ionic Crystals," Paraday Society Transactions, XLVIII (January, 1949), 155-166.
- Tyagai, V. A., "Study of the Nature of a Pulsed Photo-effect at a Cadmium Sulfide-Electrolyte Solution Interface," Soviet Physics-Solid State, VI (December, 1964), 1260-1264.
- Vermilyea, D. A., "The Dissolution of Ionic Compounds in Aqueous Media," Journal of the Electrochemical Society, CXIII (October, 1966), 1067-1070.
- Williams, R., "Electrical Effects of the Dissolution of n-Type Zinc Oxide," Journal of Applied Physics, XXXIX (August, 1968), 4089-4091.